Title Page

Thinopyrum intermedium TiAP1 interacts with a chitin deacetylase from *Blumeria graminis* f. sp. *tritici* and increases the resistance to *Bgt* in wheat

Yanlin Yang[1], Pan Fan[1], Wenjun Xie[2], Na Liu[1], Zubiao Niu[1], Quanquan Li[1], Jing Song[1], Qiuju Tian[1], Jingxia Liu[1], Yinguang Bao[1], Honggang Wang[1], Deshun Feng[1,*]

1. State Key Laboratory of Crop Biology, Shandong Key Laboratory of Crop Biology, College of Agronomy, Shandong Agricultural University, Tai'an 271018 Shandong, China;
2. Plant Defence Genetics Lab, Department of Plant and Environmental Sciences, University of Copenhagen, Thorvaldsensvej 40, Frederiksberg C, Denmark

Author for correspondence:

Deshun Feng

Tel: +86 538 8246821

Email: dsfeng@sdau.edu.cn

Thinopyrum intermedium TiAP1 interacts with a chitin deacetylase from *Blumeria graminis* f. sp. *tritici* and increases the resistance to *Bgt* in wheat

Yanlin Yang[1], Pan Fan[1], Wenjun Xie[2], Na Liu[1], Zubiao Niu[1], Quanquan Li[1], Jing Song[1], Qiuju Tian[1], Jingxia Liu[1], Yinguang Bao[1], Honggang Wang[1], Deshun Feng[1,*]

1. State Key Laboratory of Crop Biology, Shandong Key Laboratory of Crop Biology, College of Agronomy, Shandong Agricultural University, Tai'an 271018 Shandong, China;
2. Plant Defence Genetics Lab, Department of Plant and Environmental Sciences, University of Copenhagen, Thorvaldsensvej 40, Frederiksberg C, Denmark

* Correspondence: dsfeng@sdau.edu.cn (D.F.); Tel.: +86-0538-8246821(D.F.)

Summary

The biotrophic fungal pathogen *Blumeria graminis* f. sp. *tritici* (*Bgt*) is a crucial factor causing reduction of global wheat production. Wild wheat relatives, e.g. *Thinopyrum intermedium,* is one of the wild-used parents in wheat disease-resistant breeding. From *T. intermedium* line, we identified the aspartic acid protein gene, *TiAP1*, which involved in resistance against *Bgt*. TiAP1 is a secreted protein that accumulates in large amounts at the infection sites of powdery mildew and extends to the intercellular space. Yeast two-hybrid showed that it interacted with the chitin deacetylase (BgtCDA1) of *Bgt*. Host-induced gene silencing showed *BgtCDA1* promotes the invasion of *Bgt*. Transcriptome analysis showed the cell wall xylan metabolism, lignin biosynthesis-related, and defence genes involved in the signal transduction were upregulated in the transgenic *TiAP1* wheat induced by *Bgt*. The TiAP1 in wheat may inactivate BgtCDA1 deacetylation function, cause chitin oligomers expose to wheat chitin receptor, then trigger the wheat immune response to inhibit the growth and penetration of *Bgt*, and thereby enhance the tolerance of wheat to pathogens.

Key words:

Blumeria graminis f. sp. *tritici*, chitin deacetylase, disease resistance, *Thinopyrum intermedium*, *TiAP1*, wheat

Introduction

Wheat (*Triticum aestivum* L.) is one of the main crops in the world, therefore the production of wheat is closely related to food security. In recent years, pathogenic infections have seriously affected the yield of wheat. Wheat powdery mildew caused by the obligate biotrophic fungus *Blumeria graminis* f. sp. *tritici* (*Bgt*) can result in severe reductions in grain yield (Singh *et al*., 2016). When powdery mildew invades the plant, the plant responds immediately to the pathogen invasion (Geziel, 2015). During this process, the powdery mildew releases proteinaceous exudates that contain the mechanical and molecular features required for the full virulence of the pathogen (Zhang *et al*., 2005). Fungal exudates function in the attachment of conidia and in the adherence of the penetrating appressoria (App) to invade plants (Deising *et al*., 2000).

So far, there are few studies examining the infection mechanism of the wheat powdery mildew. In wheat, more than 66 powdery mildew resistance loci (*Pm1-Pm66*) located on different chromosomes of the common wheat have been named (Li *et al*., 2020a). Most of them originated from wild relative species of wheat, such as *Pm21* from *H. villosa* has been introduced into the common wheat using the translocation line T6VS·6AL (Chen *et al*., 2013). Li *et al*. (2020b) cloned *Pm41*, which was a powdery mildew resistance gene deriving from the wild emmer wheat. *Thinopyrum intermedium* had been hybridized extensively with wheat and proven a useful source of resistance to various diseases of hexaploid wheat (Shen *et al*., 2015). The mining and utilization of these new resistance genes are vital means to improve current wheat varieties and increase their resistance to powdery mildew.

Aspartic proteases consist of four main proteolytic enzymes that are widely present in animals, plants, yeast, microorganisms, and viruses (Rawlings and Barrett, 1995). Xia *et al*. (2004) reported that the peptide signal system of CDR1 was involved in the activation of the resistance mechanism, while Prasad *et al*. (2009, 2010) found that *OsCDR1/OsAP5* could enhance the disease resistance of rice and *Arabidopsis thaliana*. The aspartic protease gene, *AP13*, from grape could promote the salicylic acid-dependent signal transduction pathway (Guo *et al*., 2016). Moreover, Alam *et al*. (2014) found that the rice *OsAP77* gene accumulated in the extracellular space and sieve tubes to defend the pathogens. Hence, these studies have shown aspartic proteases participate

in the biotic stresses of plants to enhance the resistance.

To resist pathogens, plants have developed a complex immune system including the plasma membrane receptors that recognise pathogen-related molecular patterns, such as chitin from the fungal cell walls that can trigger defence responses. Kamakura *et al*. (2002) found a new germination tube-specific gene, *CBP1*, in the rice blast fungus *Magnaporthe grisea*. This gene encodes a chitin-binding protein (CBP) having two similar chitin-binding domains at both sides of the central domain. This structure is similar to the fungus chitin deacetylase, which may play a vital role in the hydrophobic surface sensing of *M. grisea* during App differentiation. Kuroki *et al*. (2017) confirmed *CBP1* encoded a chitin deacetylase and participated in differentiation stage of App in *M. oryzae*. These results proved the chitin deacetylase activity of CBP1 is necessary for the formation of App. In addition, Yang *et al*. (2019) identified the chitinase gene *MoChia1* from *M. oryzae*. This gene can trigger a plant's defence response to *M. oryzae* in rice under an inducible promoter. MoChia1 was also a functional chitinase that is required for the growth and development of *M. oryzae*. The MoChia1 binding to free chitin could inhibit the plant immune response, while another protein, OsTPR1, competitively binding with MoChia 1, would re-establish the immune response (Yang *et al*., 2019). Han *et al*. (2019) also found the mechanism of MoChi1 that targeted the host lectin to inhibit rice immunity and promote the colonisation. Furthermore, they also found rice protein OsMBL1 could interact with MoChi1 to enhance the resistance against *M. oryzae*. Overexpressing of *OsMBL1* can lead to the activation of defence response genes of rice and the burst of chitin-induced reactive oxygen species (ROS). Moreover, Gao *et al*. (2019) identified a secreted polysaccharide deacetylase (PDA1) from soil-borne *Verticillium dahliae*. PDA1 can promote the deacetylation of chitin oligomers, whose *N*-acetyl group contributes to the host lysine motif (LysM)-containing receptor that perceives ligand-triggered immunity and facilitates virulence. Thus, the silencing of PDA1 allows the N-acetyl group of the chitin-triggered host immunity to occur.

In a previous study, we obtained an aspartic protease gene, *TiAP1*, from trititrigia SN6306 through a comparative transcriptome analysis. Further sequence analysis

showed *TiAP1* originated from *T. intermedium* (Tian *et al*., 2017). Through gene expression and virus-induced gene silencing (VIGS) analyses, we found the *TiAP1* gene might be involved in the resistance to wheat powdery mildew. In addition, Subcellular localisation analysis showed that TiAP1 is of a secretory protein. During the powdery mildew invasion, TiAP1 would assemble in large numbers at the infect site. The yeast two-hybrid (Y2H) verification, luciferase (LUC) complementation imaging (LCI), Co-Immunoprecipitation (Co-IP) and bimolecular florescent complimentary (BiFC) analysis show that TiAP1 interacts with chitin deacetylase (BgtCDA1) of *Bgt*, while BgtCDA1 could promote the invasion of *Bgt*. Therefore, we propose that TiAP1 induces the plant to resist the invasion of pathogens by interacting with BgtCDA1, which makes the chitin of the fungus inherently immune to the plant.

Results

The expression of *TiAP1* mediates the *Bgt*- resistance in trititrigia SN6306 to *Bgt* invasion

Li *et al*. (2016) analyzed the transcriptome of SN6306 and YN15 and obtained a gene that was upregulated by *Bgt* induction, which encoded an aspartic protease. Tian *et al*. (2017) cloned the *TiAP1* gene and found that it came from *T. intermedium*. Here, we found that the *TiAP1* gene was expressed in SN6306 rather than in wheat YN15, and it was upregulated by the *Bgt*-induced in the early stages of the Bgt invasion (Fig. 1A).

To investigate the effect of endogenous *TiAP1* on SN6306 resistance to *Bgt*, we reduced the endogenous *TiAP1* gene levels by suppressing *TiAP1* expression using BSMV-VIGS. The *TiAP1* expression levels were significantly suppressed in the leaves of BSMV: TiAP1as SN6306 relative to the BSMV: 00 negative control (Fig. 1B). When the BSMV: TiAP1as SN6306 was inoculated with *Bgt* at the two-leaf stage, the infection in BSMV: TiAP1as SN6306 was much more severe than in the BSMV: 00 control at 10 days post-inoculation (dpi) (Figs. 1C, 1D). This proved that the *TiAP1* gene was resistant to *Bgt* invasion and could play a role in the resistance.

The TiAP1 protein enhances resistance to *Bgt in vitro*

Western blot analysis showed that TiAP1 was induced in the precipitation (Figs. 2A, 2B, S1). After renaturation, the protein concentration was determined to be 0.437

155 mg/mL by the Bradford method (Fig. 2C; Bradford, 1976). Moreover, regarding the
156 TiAP1 expression effect on the *Bgt* invasion, the number of *Bgt* conidia on YN15 leaf
157 after smearing TiAP1 for 5 days was significantly lower than that of YN15 with CK
158 (pET28a). In addition, there was a small number of hyphae in the leaves smeared with
159 TiAP1, where the hyphal length and the diseased area were less than those of the leaves
160 smeared with CK (Figs. 2D, 2E). Lesion areas of the leaves treated with TiAP1 were
161 also significantly less than that of the control (Fig. 2F), suggesting that TiAP1 can resist
162 the *Bgt* invasion *in vitro*.

163 ***TiAP1* gene transfer can elevate the resistance to *Bgt* of the recipient wheat**

164 To investigate the function of *TiAP1*, the pMUbi-*TiAP1* vector and the screening marker
165 *Bar* gene vector, were co-transformed into the susceptible hexaploid wheat cultivar,
166 Bobwhite. The obtained transgenic Bobwhite with the *TiAP1* gene were subjected to
167 PCR identification of the *Bar* and *TiAP1* genes (Figs. S2A, S2B) to obtain the positive
168 transgenic plants. The qRT-PCR analysis showed that the expression level of the *TiAP1*
169 gene was higher in OE1 and OE2 of SN6306 when infected by *Bgt* 2 dpi, respectively.
170 After multiple comparisons, we found that the expression level of *TiAP1* when infected
171 by *Bgt* in OE2-2 was significantly different from that of OE2-0 ($P < 0.05$) (Fig. 3A),
172 indicating that the expression of *TiAP1* could be involved in the interaction with *Bgt*.
173 In addition, we found that the overexpression of *TiAP1* gene in Bobwhite (OE1 or OE2)
174 showed moderate resistance, while the leaf surface was still entirely green and less
175 conidia were present at 5 dpi than the control Bobwhite (Fig. 3B). Moreover, there were
176 a large number of conidia in Bobwhite that had germinated and formed hyphae 2 dpi
177 using *Bgt*. A large number of conidia in the OE1-2, OE2-2 and SN6306 were retained
178 at App of 41.2 %, 43.4 % and 83.7 %, and 16.2 %, 14.5% and 0.34 % retained at hyphae
179 stage, respectively, while in the control Bobwhite, 28.9 % of the conidia were present
180 in the form of App and 25.6 % of the conidia were present in the form of hyphae (Figs.
181 3C, 3D). The HI in Bob-2 was 68.6%, while in OE1-2, OE2-2 and SN6306 it was
182 48.8 %, 53.5 % and 6.7 %, respectively (Fig.3F). In addition, figures 3D and 3E
183 suggested that the transgenic *TiAP1* gene could affect the formation of *Bgt* Hau, thereby
184 resisting the invasion of *Bgt*.

185 Meanwhile, we crossbred between the homozygous transgenic *TiAP1* Bobwhite and
186 YN15 to obtain the hybrid F_1. Gene amplification and phenotype investigation
187 confirmed the inheritance of the *TiAP1* gene and its function in resisting *Bgt* in the
188 hybrid F_1. A chi-square test showed that the proportion of resistant-susceptible
189 separation in the F_2 generation was 3:1. The subsequent F_3 generation at the seedling
190 stage (Figs. S2C, S3; Table S1) also double confirmed *TiAP1* endue the resistance to
191 *Bgt* for wheat.

192 In the adult stage, through natural infection by powdery mildew in the glasshouse,
193 the overexpression of *TiAP1* gene in Bobwhite showed high resistance to *Bgt* (Figs.
194 3F2, S4; Table S2), whereas Bobwhite (Fig. 3F1) and YN15 (Fig. 3F3) showed high
195 susceptibility to *Bgt* on the leaves with many lesions of more than 1 mm in diameter
196 and more hyphae. At the same time, the hybrid F_1 between the overexpression of *TiAP1*
197 gene in Bobwhite and YN15, showed high resistance to *Bgt*, where the diameter of the
198 lesions was less than 1 mm, the amount of the leisons was little, the whole leaf surface
199 was still green (Fig. 3F4). .

200 **TiAP1 is a secretory protein that accumulates at the infection site**

201 To determine the localisation of TiAP1 in plant cells, we utilised the TiAP1-GFP, Δsp-
202 TiAP1-GFP, and free GFP transient transformation in *N. benthamiana*. Through
203 plasmolysis methods, we found that the fluorescent signals of TiAP1-GFP were outside
204 the cell membrane, while Δsp-TiAP1-GFP (without signal peptide) was in the
205 cytoplasm (Figs. 4A, 4B, 4C, S5). To further confirmation whether TiAP1 is a secretory
206 protein, the mCherry-TaSYP51, which is a member of the syntaxin superfamily on
207 plasma membrane, was co-bombarded with TiAP1-mYFP into the barley leaf epidermal
208 cells. We found a large numbers TiAP1 and TaSYP51 proteins accumulated at the
209 infection site of the primary and App germination tube of *Bgh*, and TiAP1 extended to
210 the barley intercellular space (Fig. 4D; Video S1). Integrating with our observations of
211 the *Bgt* on the leaves of *TiAP1* gene transferred wheat, we speculated that TiAP1
212 restrains the powdery mildew from penetration, assisting the plants in resisting the
213 invasion of *Bgt*.

214 **The BgCDA1 interact with TiAP1**

215 To clarify how TiAP1 can regulate wheat resistance to *Bgt*, CDS of TiAP1 without
216 signal peptide was fused with the GAL4 DNA-binding domain sequence to generate
217 the bait vector. We performed a Y2H screen assay using *Bgt* cDNAs as a prey library.
218 Interestingly, one of the obtained interactors with highly similar (95.06%) to the chitin
219 deacetylase (EPQ66796.1) of *Bgt*. Furthermore, the analysis of the cDNA revealed that
220 the related protein contains a polysaccharide deacetylation domain. Therefore, we
221 named this gene chitin deacetylase (*BgtCDA1*) of *Bgt* (Figs. S6A, S6B). The BgtCDA1
222 has an N-terminal 19-aminoacid signal peptide
223 (http://www.cbs.dtu.dk/services/SignalP) and five conserved motifs that are required
224 for hydrolysing the acetyl groups of the substrates (Figs. S6C, S6D). Moreover, the
225 point-to-point verified the BgtCDA1 without signal peptide fused to the GAL4
226 activation domain interact with TiAP1 (Fig. 5A).

227 Subsequently, we furtherly confirmed the interaction through LCI, Co-IP and BiFC.
228 As expected, the LUC activity in the *N. benthamiana* leaves was high when co-injected
229 using the ΔspTiAP1-nLuc and ΔspBgtCDA1-cLuc, while the other three combinations
230 were used as negative controls (Fig. 5B). The Co-IP analysis showed that TiAP1
231 interacts with BgtCDA1, and when BgtCDA1 and TiAP1 were expressed together, the
232 amount of BgtCDA1 was less than that it expressed alone (Fig. 5C). The BiFC analysis
233 also confirmed that the co-expression of nGFP-ΔspBgtCDA1 and cGFP-ΔspTiAP1
234 resulted in a clear GFP signal in the cytoplasm. In contrast, no visible signal was
235 detected in any of the corresponding negative controls (Fig. 5D). Therefore, these
236 observations indicate that there is an *in vivo* interaction between TiAP1 and BgtCDA1.

237 **HIGS analysis showed that the silencing of *BgtCDA1* inhibits the penetration and**
238 **Hau formation of *Bgt***

239 To confirm the role of *BgtCDA1* in the growth and development of *Bgt*, we used a
240 transient transformation system based on the particle bombardment of RNAi constructs
241 (Douchkov *et al*., 2005). Through statistical analysis, we found that after the
242 normalization treatment, the HI of the positive control, Mlo-RNAi, was 47.44%, while

243 that of *BgtCDA1* RNAi was 55.36% (Fig. 6A, 6B). And through BSMV-VIGS, we also
244 found that the lesions area in the leaves of BSMV: BgtCDA1as wheat infected with
245 powdery mildew for 5 days and the hyphal density score of powdery mildew infection
246 for 3 days were significantly lower than those of BSMV:00 wheat (Figs. 6C, 6D, 6E,
247 6F). This indicated that *BgtCDA1* gene silencing suppressed the growth of powdery
248 mildew conidia and the *BgtCDA1* gene promoted the invasion of *Bgt*.

249 **TiAP1 and BgtCDA1 co-regulate the expression of wheat pathogen-responsive**
250 **genes**

251 To evaluate the impact of TiAP1 and BgtCDA1 on the pathogen-responsive gene
252 expression on a genome-wide scale, we performed RNA-Seq experiments using
253 Bobwhite and OE2 seedlings inoculated with *E09* for two days (Fig. S7A). Genes with
254 more than a four-fold change in expression ($P < 0.01$) were considered to be
255 differentially expressed. Total 274 differentially expressed genes were detected in the
256 OE2-2-vs-Bob-2 after 2 dpi, of which 116 genes were upregulated when inoculated
257 with *E09* in the OE2-2 (Figs. S7B, S7C; Table S3). Gene ontology (GO) analysis
258 indicated that these differentially expressed genes were enriched in the chitin catabolic
259 process, cell wall macromolecule catabolic process, defence response to bacterium and
260 fungus, chitinase activity, and chitin-binding (Fig. S7D; Table S4). Defence-related
261 genes were also upregulated in OE2-2 relative to Bob-2, such as *traesCS1A02G410500*,
262 *traesCS2B02G187500*, *traesCS2A02G161500*, *traesCS3B02G379200* and
263 *traesCS1B02G440300* that encode proteins containing WRKY domains;
264 *traesCS5A02G049600*, *traesCS7A02G201100*, *traesCS5D02G188600*,
265 *traesCS6D02G217800* and *traesCS3A02G404400* that are related to plant hormone
266 signal transduction; *traesCS6B02G018700* that encode a 4,5-DOPA dioxygenase
267 extradiol gene that is involved in betaine metabolism; *traesCS5A02G203500*,
268 *traesCS6B02G0183700* and *traesCS5A02G02G0183700* that are ubiquitin E3 ligase
269 RING-type related genes; and *traesCS6A02G266100* that encode the xyloglucan
270 glycosyltransferase/hydrolase involved in cell wall xylan metabolism (Fig. 7A; Table
271 S5). By qRT-PCR, we further analysed twelve gene which was differential expression

induced of *Bgt* for two days. Among these twelve genes, the expression levels of *TraesCS1B02G440300*, *TraesCS2A02G161500*, *TraesCS2A02G199300,* TraesCS*3B02G379200, TraesCS5D02G188600* and *TraesCS5A02G049600* which related to plant hormone signal transduction were all upregulated in OE2-2 relative to Bob-2, beside *TraesCS5D02G188600* which was no difference in OE2-2 relative to Bob-2 (Fig 7B). The *TraesCS3B02G259500*, *TraesCS2B02G224300*, *TraesCS6A02G266100* and *TraesCS2D02G099900* involved in cell wall anabolism, in which *TraesCS3B02G259500* and *TraesCS6A02G266100* were consistent with transcriptome were upregulated in OE2-2 relative to Bob-2, *TraesCS2B02G224300* and *TraesCS2D02G099900* were no difference in OE2-2 relative to Bob-2, but the expression in OE2-2 was higher than Bob-2, and *TraesCS6B02G018700* and *TraesCS2B02G529400* genes expression pattern were similar with *TraesCS2B02G224300* and *TraesCS2D02G099900* (Fig. 7B).These quantitative results were slightly different to those at the transcriptome, possibly because of the differences between individuals. In summary, the upregulated expression of these genes provided favourable evidence to understand the disease resistance mechanism of the *TiAP1* gene.

Discussion

Aspartic proteases play a vital regulatory role in plant growth and may be involved in the senescence process (Chen *et al*., 2015), plant reproduction (Niu *et al*., 2013), programmed cell death (Chen and Foolad, 1997), resistance to pathogens (Prasad *et al*., 2010), response to stress (Guo *et al*., 2013) and endoproteases in plants (Rawlings *et al*., 2016). If the endoproteases encoding genes were deleted or inhibited, the plant's sensitivity to pathogens increases (Jashni *et al*., 2015; Díaz *et al*., 2018). In the early stage, our laboratory cloned an aspartic protease gene *TiAP1* which was originated from *T. intermedium* (Tian et al., 2017). Sequence analogical analysis showed that the *TiAP1* was most similar to wheat aspartic protease gene *TaAP207* (TraesCS5D02G083000.1) among all the predicted *TaAPs,* with 70% identity. But *TaAP207* wasn't found to express highly under *Bgt* invasion (Yang and Feng 2020). The qRT-PCR analysis showed that the *TiAP1* gene was rapidly expressed under the induction of *Bgt* in

301 SN6306 with no expression in YN15 (Fig. 1A). *TiAP1* expression levels were
302 significantly suppressed with more hyphae piles appearing in the leaves of BSMV:
303 TiAP1as SN6306 (Figs. 1B–1D) as well as lesion areas on the leaves that were smeared
304 with the TiAP1 protein level when compared to the control (Figs. 2D–2F). These results
305 indicated that *TiAP1* might resist the invasion of powdery mildew.

306 Furthermore, the identification of the *Bgt* resistance phenotype at the seedling stage
307 showed that the overexpression of *TiAP1* gene in wheat was moderately resistant to
308 powdery mildew (Fig. 3B), while the life cycle of *Bgt* in the two-day-infected leaves of
309 the overexpression of *TiAP1* gene in Bobwhite was primarily retained in the App stage.
310 In contrast, the conidia on the Bobwhite leaves were mainly in Hau stage. Hau was
311 wrapped in the extrahaustorial membrane (EHM), which was usually used for signal
312 exchange and nutrient absorption (Panstruga, 2013), where the development of the Hau
313 reflected the growth and metabolism of the entire pathogen to a certain extent. It was a
314 vital trait for evaluating host cell resistance (Bracket, 1968).

315 The HI of *Bgt* in Bobwhite was significantly higher than that of the transgenic *TiAP1*
316 gene lines, indicating that overexpression of *TiAP1* gene in Bobwhite could resistance
317 to the *Bgt* invasion (Fig. 3E). This resistance may be because the transgenic wheat
318 inhibited the penetration of the powdery mildew, thereby affecting their infection rate.
319 Subsequently, we found that the transgenic *TiAP1* Bobwhite and the F_1 generation
320 showed high resistance to powdery mildew in the adult-stage (Figs. 3F2, 3F4, S4).
321 Many studies refer to this trait, which showed less significant resistance to the disease
322 at the seedling stage than that of the adult stage (Hautea *et al*., 1987; Griffey and Das,
323 1994), or of a chronic disease resistance type (Shaner, 1973). Moreover, Shaner (1973)
324 found condia of Konx, a typical slow-white powder variety, could not successfully
325 invade. Therefore, we speculated that the transgenic wheat line with the *TiAP1* gene
326 might be used as a chronic powdery mildew-resistant variety to prevent the invasion of
327 *Bgt*. Syntaxins were members of the SNARE superfamily of proteins that mediated
328 membrane fusion events (Colline *et al*., 2003). Since TiAP1 was a secreted protein (Figs.
329 4A, 4B, 4C) which expressed in large quantities at intercellular space of the infection
330 site (Fig. 4D, Video S1), we speculate that syntaxin TaSYP51 may help to transport the

331 TiAP1 protein to the outside of the cell, where the detailed mechanisms need to be
332 further elucidated.

333 Through the Y2H, LCI, Co-IP, and BiFC *in vivo* verification, we determined TiAP1
334 interacts with BgtCDA1 (Fig. 5). Subsequently, we found that when the *BgtCDA1* gene
335 was silenced, the HI, lesions area and hyphal density score were significantly reduced
336 (Fig. 6). Similarly, Zhao *et al*. (2010) found that chitin deacetylase was secreted when
337 it interacted with other substances. The chitin deacetylase of *C. lindemuthianum* was
338 secreted during the process of fungal hyphae invading plants to modify the chitin that
339 can be recognised by the plant's resistance system (Tsigos and Bouriotis, 1995).
340 Geoghegan and Gurr (2017) also found in *M. oryzae* that CDA1 and CDA4 were
341 necessary for chitin deacetylation in the cell wall of the mycelium. During infection,
342 the ability of the fungal cells to convert chitin to chitosan was critical for masking the
343 cell wall chitin from being recognised by the host chitinases, thereby promoting the
344 fungal attack (Upadhya *et al*., 2018). Chitin oligomers can also act as ligands that were
345 recognised by LysM receptors on the cell surface and triggered pathogen-associated
346 molecular pattern (PAMP)-triggered immunity (PTI) (Hurlburt *et al*., 2018; Gao *et al*.,
347 2019). The silencing of *BgtCDA1* could inhibit the invasion of *Bgt* and we speculated
348 that the interaction between BgtCDA1 and TiAP1 made BgtCDA1 be degraded by
349 TiAP1, which inhibited the deacetylation function of BgtCDA1. Moreover, the growth
350 and penetration of *Bgt* was inhibited and the chitinase of the wheat was secreted to
351 release the chitin oligomers, which were recognised by the wheat chitin receptor, such
352 as LysM. This led to PTI and caused the transgenic wheat with the *TiAP1* gene to be
353 resistant to powdery mildew (Fig. 8). When the pathogen invades the host, an extremely
354 complex and precise arms race of 'attack and defence' occurs in the apoplastic space.
355 Xia *et al*. (2020) also proposed a 'multi-layered immune model' of the plants against
356 pathogens in the extracellular region when studying the mechanism of action of
357 PsXEG1 against *Phytophthora sojae*. Therefore, this study revealed the complexity of
358 the interaction between pathogens and hosts as well as provided a theoretical basis to
359 further study the role of TiAP1 in resistance mechanisms.

360 When chitin receptors recognise the chitin, the plant can active defence genes and

361 release some metabolites that initiate the signal transduction in plant cells to trigger an
362 immune response. The metabolites include abscisic acid, ethylene, jasmonic acid,
363 gibberellic acid, and ubiquitination that caused the plants to respond to the invasion of
364 pathogens (Fig. 7; Table S3). Moreover, RNA-Seq and qRT-PCR analysis revealed that
365 there was a cell wall xylan metabolism gene, *traesCS6A02G266100*, whose expression
366 in Bobwhite was sharply reduced after being induced by powdery mildew, while the
367 gene in OE2-2 was significantly upregulated relative to that of Bob-2 (Fig. 7).

368 Since xylan was a type of hemicellulose that was closely related to functional
369 proteins in the cell wall, it had a great influence on the ductility, pore elasticity, flow,
370 and rheological properties of plant cells during growth (Zhou *et al*., 2017). Therefore,
371 we infer that the penetration during the powdery mildew infection of the transgenic
372 wheat with the *TiAP1* gene was blocked. We also found that the *TraesCS2B02G224300*
373 gene encoded a phenylalanine ammonia-lyase (PAL), which was upregulated and
374 significant difference in OE2-2 relative to Bob-2 in transcriptome (Fig. 7A; Table S5),
375 and in qRT-PCR the expression of *TraesCS2B02G224300* in OE2-2 was twice higher
376 than Bob-2 (Fig. 7B). The PAL was pivotal for the enzymes related to the biosynthesis
377 of lignin, salicylic acid, and other phenylalanine-derived metabolites (You *et al*., 2020).
378 As a main component of the plant cell wall, lignin contributes to the formation of the
379 physical and chemical barriers in the plant immunity. Zhou *et al*. (2018) also found that
380 *OsPAL1*-mediated resistance to rice blast might be due to the accumulation of lignin,
381 while the broad-spectrum blast-resistant rice varieties *Pigm*- and *PIBP1*-mediated
382 resistance might be related to lignin content (Zhai *et al*., 2019). Similarly, the
383 overexpression of *OsPAL8* in rice can lead to increased lignin content and enhanced
384 brown plant hopper resistance (He *et al*., 2020). Thus, these results demonstrate that the
385 transgenic wheat with the *TiAP1* gene could enhance resistance to *Bgt.*

386 In summary, we speculate the fungal chitin deacetylase BgtCDA1 can block the
387 PAMP processes that the fungal derived chitin oligoes are recognized by wheat chitin
388 receptor protein and then trigger an immune response, while TiAP1 competitively
389 interacting with BgtCDA1 is the causal reason to re-establish resistance to fungal
390 pathogen *Bgt*. Moreover, the interaction between TiAP1 and BgtCDA1 upregulates the

391 cell wall-related genes in transgenic *TiAP1* wheat thereby blocks the penetration of
392 powdery mildew and enhances the tolerance to pathogens. Furtheremore, we conclude
393 many other plants may share similar mechanism and this mechanism can be used for
394 future genetic improvement of crops.

395 **Materials and methods**

396 **Plant material and pathogen infection**

397 The trititrigia SN6306 was highly resistant to the powdery mildew and obtained by
398 hybridisation between the highly susceptible to powdery mildew wheat (*Triticum*
399 *aestivum* L.) cultivar Yannong 15 (YN15) and *T. intermedium* (Li *et al*., 2016). Wheat
400 Bobwhite were highly susceptible to the powdery mildew. The transgenic
401 overexpression *TiAP1* in Bobwhite line 1 and 2 were named as OE1 and OE2,
402 respectively. The untreated with *Bgt* wheat lines Bobwhite, OE1 and OE2 were named
403 as Bob-0, OE1-0 and OE2-0, respectively. The Bobwhite, OE1 and OE2 wheat
404 inoculated with *E09* for two days were named as Bob-2, OE1-2 and OE2-2, respectively.
405 The seeds of these materials above and *Nicotiana benthamiana* were sown in a mixed
406 soil (loess, matrix, and vermiculite of 1:1:1, *v*/*v*/*v*) at 25°C, 70% humidity, and a long-
407 term photoperiod of a 16 h/8 h light/dark cycle in a glasshouse with a light intensity of
408 600 mmol $m^{-2}s^{-1}$. The virulent isolate *E09* of the wheat powdery mildew fungus (*Bgt*)
409 was propagated on the wheat variety YN15 via a weekly inoculum transfer. The barley
410 (*Hordeum vulgare* L.) line Ingrid *ror2* (Collins *et al*., 2003) was highly susceptible to
411 *Blumeria graminis* f. sp. *hordei* (*Bgh*) and used for the localisation and expression
412 profiling of *TiAP1*. The *Bgh* isolate B103 was propagated on barley P-10 via a weekly
413 inoculum transfer, while the *Escherichia coli* (*E. coli*) strain BL21 (DE3) was used for
414 the prokaryotic expression of TiAP1.

415 **VIGS, barley stripe mosaic virus (BSMV), and host-induced gene silencing**
416 **(HIGS)**

417 VIGS analysis was conducted according to Yuan *et al*. (2011) to insert the conserved
418 sequence of the target *TiAP1* and *BgtCDA1* gene (316 bp and 300 bp, respectively) into

419 the BSMV vector to create BSMV: TiAP1as and BSMV: BgtCDA1as and transform the
420 *Agrobacterium*. The detailed method was described in Methods S1. Ten days after
421 inoculation with BSMV, 6 leaves were harvested to test the expression level of *TiAP1*
422 and *BgtCDA1* gene, while the other 6 leaves were inoculated with *Bgt* race *E09* and
423 were observed and used to evaluate the resistance to the powdery mildew using a
424 biological microscope (Nikon Ni-U, Japan) after the Coomassie Brilliant Blue staining
425 and the statistics of hyphal density score refer to the method of Norriss et al. (2007) and
426 three biological replicates.

427 *BgtCDA1* gene silencing in *Bgt* was performed using the HIGS method as
428 described by Nowara *et al*. (2010). The RNA interference (RNAi) construct BgtCDA1
429 RNAi and a β-glucuronidase (GUS) reporter gene construct were co-transformed into
430 the leaf epidermal cells of the wheat YN15 that grew for seven days using particle
431 bombardment. The fungal haustorial formation was examined for the transformed
432 (GUS expressing) blue cells using a biological microscope (Nicon Ni-U, Japan). The
433 empty vectors pIPKTA30N, and the Mlo-RNAi (pIPKTA36) constructs, were used as
434 negative and positive controls, respectively and four biological replicates were
435 conducted per analysis with three technical replicates. The detailed method was
436 described in Methods S1 according to Ahmed (2015).

437 **Constructing the TiAP1 prokaryotic expression plasmid and the protein**
438 **expression**

439 To improve the expression of *TiAP1*, the gene sequence was optimised according to *E.*
440 *coli* bias, and constructed into the pET28a vector (containing 6xHis tags). Recombinant
441 plasmids were transformed into BL21 (DE3) chemically competent cells where a
442 single-colony transformant was cultured and inoculated at 15 °C overnight induced
443 expression with 0.25 mM isopropyl β- d-1-thiogalactopyranoside (IPTG). The cells
444 were harvested and subjected to a sodium dodecyl sulphate-polyacrylamide gel
445 electrophoresis (SDS-PAGE) to detect the protein expression. Then, the recombinated
446 TiAP1 was purified according to the method described in Methods S1.

447 **Determination of the antifungal activity of TiAP1**

448 To confirm the effect of TiAP1 protein on *Bgt*, we used the renatured TiAP1 and
449 pET28a tag protein to add 0.025% Tween-20 to smear the leaves of YN15 and inoculate
450 with *E09*. After five days, the infectivity of *Bgt* was observed and the leaves were
451 stained with the Coomassie Brilliant Blue stain, as described previously (Göllner *et al*.,
452 2008) and three biological replicates were conducted per analysis with three technical
453 replicates. Lesion areas on the leaf surface were calculated according to Goodwin and
454 Hsiang (2010) to analyse the pixels of the *Bgt* infection area relative to the normal leaf
455 area.

456 **Constructing the particle bombardment genetic transformation vector to**
457 **transform wheat and identify the disease resistance phenotype**

458 The coding sequence (CDS) of *TiAP1* (KJ513672) was cloned into the *Ubi-gene*-Tnos
459 vector with a ubiquitin (Ubi) promoter, yielding a recombinant pMUbi-*TiAP1* vector.
460 The resulting plasmid pMUbi-*TiAP1* and the vector harboring the *Bar* gene were mixed
461 and co-bombarded with a particle bombardment of 1100 psi, 1 μg per gun, and 60 μg
462 gold powder into the callus that was induced from the mature embryos of the Bobwhite
463 wheat, which was highly susceptible to *Bgt*. During the induction and regeneration, the
464 transformed wheat was screened using the herbicide Basta, while the presence of the
465 transgenes was determined by amplifying the target gene using the pUbi-ASPF/R
466 primers (Table S6).

467 Next, the disease responses to powdery mildew of the transgenic plants were tested.
468 When the Bobwhite and the transgenic Bobwhite with the *TiAP1* gene grew to the three-
469 leaf stage, the first leaves of them were spread out on an acrylic plate with the conidium
470 of the *Bgt* race *E09* sprayed evenly. The leaves were harvested at 48 h post-inoculation
471 with *E09* and stained with Coomassie Brilliant Blue as described previously (Göllner
472 *et al*., 2008) and three biological replicates were conducted per stains with three
473 technical replicates. Furthermore, to evaluate the resistance to *Bgt* of the Bobwhite and
474 the transgenic Bobwhite with the *TiAP1* gene in the adult stage, they were natural
475 infected by powdery mildew, where the infection type (IT) of each plant was scored as
476 described by Lu *et al*. (2020).

477 **DNA and RNA extraction and qRT-PCR**

478 Total DNA was extracted from the plant leaves using the cetyltrimethylammonium
479 bromide (CTAB) method (Allen *et al*., 2006). While total RNA (500 ng) was extracted
480 using the EasyPure® Plant RNA kit (TransGen Biotech Co., Ltd, Beijing, China),
481 reverse-transcribed (RT) using a RevertAid First Strand cDNA synthesis kit (TransGen
482 Biotech Co. Ltd, Beijing, China), and quantified on an ABI Quantitative PCR Q6
483 Detection System (Thermo Fisher Scientific, USA) with the SYBR Premix Ex Taq kit
484 (TransGene Biotech Co., Ltd, Beijing, China). The wheat actin gene was used as the
485 reference gene, in which three independent biological replicates were conducted per
486 analysis with at least three technical replicates. The primers have been listed in Table
487 S6.

488 **Subcellular localisation**

489 The CDS of the *TiAP1* fragments was fused green fluorescent protein (GFP) in the
490 vector pCAMBIA1300. Then the constructed TiAP1-GFP or Δsp-TiAP1-GFP (with or
491 without signal peptide of TiAP1 respectively) were transferred into the *Agrobacterium*
492 *tumefaciens* GV3101 and transiently expressed in *N. benthamiana* leaves. Two days
493 after infiltration, they were observed using a confocal laser scanning microscope (Leica
494 SP5 - X, Germany), 10 *N. benthamiana* leaves were analyzed in each of the three
495 experiments and the detailed method was described in Methods S1.

496 **Transient expression of the TiAP1 protein induced by *Bgh* using barley leaves**

497 The expression vector of the TiAP1 protein was constructed using the gateway system
498 (Thermo Fisher Scientific, USA). The two recombinant plasmids, TiAP1-mYFP and
499 mCherry-TaSYP51, were co-bombarded onto the leaves of the 7-day-old barley by
500 particle bombardment at a helium pressure of 1,100 psi and placed on the 1%
501 Phytagel™ petri dishes containing 40mg ml^{-1} of benzimidazole (Sigma-Aldrich, USA)
502 to culture for 24 h, and then inoculated with *Bgh* spores. After additional 24 h of
503 inoculation, the expression of TiAP1 and TaSYP51 proteins were observed and
504 analysed using a confocal laser-scanning microscope (Leica SP5 - X, Germany)

according to the methodology of Smigielski *et al.* (2019). And three biological replicates were conducted per co-bombarded with six leaves.

Protein Interaction Assay

We sampled the leaves of YN15 and SN6306, which were infected with *Bgt* from 0 to 5 d, and then sent the samples to Qingdao Oebiotech Co. Ltd. (China) to construct a primary cDNA library using the BP reaction of the CloneMiner II kit (Invitrogen, Thermo Fisher Scientific, USA). Then, we identified the quality of the cDNA library. Next, we used the nuclear system Y2H mating standard operating procedure method as described in the manufacturer's instructions (Clontech Laboratories, Inc., USA) to screen the protein that interacts with TiAP1 and further verified the obtained interaction protein, and three biological replicates were conducted per Y2H verify. Then the structure, amino acid sequence domain, and the signal peptide of the obtained protein BgCDA1 were analysed using the the Basic Local Alignment Search Tool (PBLAST; Altschul *et al*., 1997), Pfam (Finn *et al*., 2014), and SignalP 5.0 (Almagro Armenteros *et al*., 2019) software, respectively.

For LCI assay, by amplifying the sequence of TiAP1 and BgtCDA1 and applying homologous recombination with the nLuc and cLuc, as previously described (Chen *et al*., 2008), the fusion protein and one of the corresponding co-injected empty vectors, nLuc/cLuc, was co-expressed in *N. benthamiana* as a negative control. At 48 h post-infiltration, the LUC activity of the leaves was observed using an *in vivo* imaging system (Berthold LB985 NightSHADE, Germany). 10 *N. benthamiana* leaves were analyzed in each of the three experiments.

For Co-IP assay, the TiAP1 and BgCDA1 protein samples were transiently coexpressed in *N. benthamiana* and the total proteins extracted from *N. benthamiana* leaves at 36 h after agroinfiltration as described above (Fiil et al., 2008). Protein extraction immunoblotting and detection were detailed performed described in Methods S1.

For BiFC assay, the sequences of TiAP1 and BgtCDA1 were amplified and fused with the N and C terminals of the GFP, respectively, using the gateway system (Thermo Fisher Scientific, USA). As mentioned previously (Bracha-Drori *et al*., 2004), the fusion protein and one of the corresponding empty GFP-N/GFP-C vectors were co-

expressed in *N. benthamiana* as a negative control. The GFP signal was observed 48 h after infiltration using a confocal laser-scanning microscope (Leica SP5 - X, Germany). 10 *N. benthamiana* leaves were analyzed in each of the three experiments.

RNA-Seq and data analysis

RNA-Seq analysis was performed using the two-leaf stage Bobwhite (Bob-0) and the transgenic Bobwhite with the *TiAP1* gene (OE2-0) as well as a Bobwhite inoculated with *E09* two days later (Bob-2) and the corresponding transgenic Bobwhite with the *TiAP1* gene (OE2-2). Three biological replicates were used for the RNA extraction, where total RNA was extracted and treated with DNase I, in which the quality test was performed, and then used to construct the library. The quality of the library was assessed using an Agilent 2100 Bioanalyzer (Agilent Technologies, Inc., USA), while the libraries were sequenced on an Illumina HiSeq 2500 platform (Illumina, Inc., USA). The RNA-Seq reads were aligned to the wheat genome of the International Wheat Genome Sequencing Consortium with the RefSeq v1.1 annotation (https://wheat-urgi.versailles.inra.fr/Seq-Repository/Annotations). Differentially expressed genes across the samples were identified using the DESeq2 package (Love *et al*., 2014) using the standard parameters with an adjusted false-discovery rate of P-value < 0.01 and fold change > 4.

Statistical analysis

The statistical significance of the results was calculated using a one-way analysis of variance followed by least significant difference and Duncan's new multiple range test at a significant difference ($P < 0.05$) using IBM SPSS software version 19.0 (Chicago, Illinois, USA). All experiments reported include three to six biological replicates and a minimum of three technical replicates with similar results. All primers have been listed in Table S6.

Accession numbers

The cDNA and coded protein sequence of *TiAP1* sequence in this research has been deposited in NCBI under the accession number KJ513672 and AJC64141.1; *Blumeria*

graminis f. sp. *tritici* BgtCDA1 was coded_by =" join (KE374986.1:122515..122759, KE374986.1:122809..123142, KE374986.1:123188..123296, KE374986.1:123342..123381, KE374986.1:123432..123502, KE374986.1:123547..123801, KE374986.1:123919..123923, KE374986.1:123978..124142, KE374986.1:124319..124375), and had one and two additional alternative splicings compared with EPQ66796 between KE374986.1:123143 and KE374986.1:123187, KE374986.1:123802 and KE374986.1:123977, respectively; Other protein sequence data from this article can be found in the NCBI under the following accession numbers: *Saccharomyces cerevisiae CDA1 (NP_013410) and Saccharomyces cerevisiae CDA2 (NP_013411).* TaSYP51 was coded by sequence in chr5A of wheat between 67321475 and 67319313.

Acknowledgements

This work was supported by the grants from the National Natural Science Foundation of China (31771777); the Key R & D program of Shandong Province (Public Welfare Special) (2018GSF121008); Shandong 'Double Tops' Program; the Major Basic Research Project of Shandong Natural Science Foundation (2017C03); and the Overseas Visiting Programme for Graduate Mentors of Shandong Province. We are very grateful to Prof. Hans Thordal-Christensen's group, University of Copenhagen, Denmark, for providing experimental assistance, to Dr. Patrick Schweizer, IPK, Gatersleben, Germany, for supplying the RNAi vector and the Mlo-RNAi construct, to Prof. Pinghua Li, Shandong Agricultural University, for providing the LCI system, and to Prof. Dawei Li, China Agriculture University, for providing the BSMV-RNAi system. Confocal image data were collected at the Center for Advanced Bioimaging (CAB), University of Copenhagen, Denmark.

Author contributions

D.F., H.W., and Y.Y. conceived and designed the experiments. Y.Y., P.F., W.X., N.L., Z.N., Q.L., J.S., Q.T., J.L. and Y.B. performed the experiments and analysed the data; Y.Y. and D.F. wrote the paper; D.F. and H.W. conceived, directed and coordinated the

project.

Competing interests

The authors have no competing interests to declare.

References

Ahmed AA, Pedersen C, Schultz-Larsen T, Kwaaitaal M, Jørgensen HJL, Thordal-Christensen H (2015) The barley powdery mildew candidate secreted effector protein CSEP0105 inhibits the chaperone activity of a small heat shock protein. *Plant Physiology* **168**: 321-333.

Alam MM, Nakamura H, Ichikawa H, Miyao A, Hirochika H, Kobayashi K, Yamaoka N, Nishiguchi M (2014) Response of anaspartic protease gene *OsAP77* to fungal, bacterial and viral infections in rice. *Rice* **7**: 1-14.

Allen GC, Flores-Vergara MA, Krasynanski S, Kumar S, Thompson WF (2006) A modified protocol for rapid DNA isolation from plant tissues using cetyltrimethylammonium bromide. *Nature Protocols* **1**: 2320-2325.

Almagro Armenteros JJ, Tsirigos KD, Sønderby CK, Petersen TN, Winther O, Brunak S, von Heijne G, Nielsen H (2019) SignalP 5.0 improves signal peptide predictions using deep neural networks. *Nature Biotechnol* **37**: 420-423.

Altschul SF, Madden TL, Schäffer AA, Zhang J, Zhang Z, Miller W, Lipman DJ (1997) Gapped BLAST and PSI-BLAST: a new generation of protein database search programs. *Nucleic Acids Research* **25**: 3389-3402.

Bracha-Drori K, Shichrur K, Katz A, Oliva M, Angelovici R, Yalovsky S, Ohad N (2004) Detection of protein–protein interactions in plants using bimolecular fluorescence complementation. *Plant Journal* **40**: 419-427.

Bracket CE (1968) The ultrastructure of the haustorial apparatus of *Erysiphe graminis* and its relationship to the epidermal cell of barley. *Phytopathology* **58**: 12-30.

Bradford MM (1976) A rapid and sensitive method for the quantitation of microgram quantities of protein utilizing the principle of protein-dye binding. *Analytical Biochemistry* **72**: 248-254.

Chen F, Foolad MR (1997) Molecular organization of a gene in barley which encodes a protein similar to aspartic protease and its specific expression in nucellar cells during degeneration. *Plant Molecular Biology* **35**: 821-831.

Chen H, Zou Y, Shang Y, Lin H, Wang Y, Cai R, Tang X, Zhou JM (2008) Firefly luciferase complementation imaging assay for protein-protein interactions in plants. *Plant Physiology* **146**: 368-376.

Chen HJ, Huang YH, Huang GJ, Huang SS, Chow TJ, Lin YH (2015) Sweet potato SPAP1 is a typical aspartic protease and participates in ethephon-mediated leaf senescence. *Journal of Plant Physiology* **180**: 1-17.

Chen P, You C, Hu Y, Chen S, Zhou B, Cao A, Wang X (2013) Radiation-induced translocations with reduced *Haynaldia villosa* chromatin at the *Pm21* locus for powdery mildew resistance in wheat. *Molecular Breeding* **31**: 477-484.

Collins NC, Thordal-Christensen H, Lipka V, Bau S, Kombrink E, Qiu JL, Hückelhoven R, Stein M, Freialdenhoven A, Somerville SC *et al*. (2003) SNARE-protein-mediated disease resistance at the plant cell wall. *Nature* **425**: 973-977.

Deising HB, Werner S, Wernitz M (2000) The role of fungal appressoria in plant infection. *Microbes and Infection* **2**: 1631-1641.

Díaz ME, Rocha GF, Kise F, Rosso AM, Guevara MG, Parisi MG (2018) Antimicrobial activity of an aspartic protease from *Salpichroa origanifolia* fruits. *Letters in Applied Microbiology* **67**: 168-174.

Douchkov D, Nowara D, Zierold U, Schweizer P (2005) A high-throughput gene-silencing system for the functional assessment of defense-related genes in barley epidermal cells. *Molecular Plant-Microbe Interactions* **18**: 755-761.

Fiil BK, Qiu JL, Petersen K, Petersen M, Mundy J (2008) Coimmunoprecipitation (co-IP) of nuclear proteins and chromatin immunoprecipitation (ChIP) from Arabidopsis. CSH Protocols pdb. prot5049. Finn RD, Bateman A, Clements J, Coggill P, Eberhardt RY, Eddy SR, Heger A, Hetherington K, Holm L, Mistry J, *et al*. (2014) Pfam: the protein families database. *Nucleic Acids Research* **42**: D222-D230.

Gao F, Zhang BS, Zhao JH, Huang JF, Jia PS, Wang S, Zhang J, Zhou JM, Guo HS (2019) Deacetylation of chitin oligomers increases virulence in soil-borne fungal pathogens. *Nature Plants* **5**: 1167-1176.

Geoghegan IA, Gurr SJ (2017) Investigating chitin deacetylation and chitosan hydrolysis during vegetative growth in *Magnaporthe oryzae*. *Cell Microbiology* **19**: e12743.

Geziel BA (2015) *On the mechanism of action of selected effector candidates from the barley powdery mildew fungus*. PhD thesis, University of Copenhagen, Copenhagen, Denmark.

Goodwin PH, Hsiang T (2010) Quantification of fungal infection of leaves with digital images and scion image software. In: Sharon A, ed. *Molecular and Cell Biology Methods for Fungi, Methods in Molecular Biology*. Springer Science+Business Media, LLC **638:**125-134.

Göllner K, Schweizer P, Bai Y, Panstruga R (2008) Natural genetic resources of *Arabidopsis thaliana* reveal a high prevalence and unexpected phenotypic plasticity of RPW8-mediated powdery mildew resistance. *New Phytologist* **177**: 725-742.

Griffey C, Das M (1994) Inheritance of adult-plant resistance to powdery mildew in Knox62 and Massey winter wheats. *Crop Science* **34**: 641-646.

Guo R, Xu X, Carole B, Li X, Gao M, Zheng Y, Wang X (2013) Genome-wide identification, evolutionary and expression analysis of the aspartic protease gene superfamily in grape. *BMC Genomics* **14**: 554.

Guo R, Tu M, Wang X, Zhao J, Wan R, Li Z, Wang Y, Wang X (2016) Ectopic expression of a grape aspartic protease gene, *AP13*, in *Arabidopsis thaliana* improves resistance to powdery mildew but increases susceptibility to *Botrytis cinerea*. *Plant Science* **248**: 17-27.

Han Y, Song L, Peng C, Liu X, Liu L, Zhang Y, Wang W, Zhou J, Wang S, Ebbole D *et*

al. (2019) A *Magnaporthe* chitinase interacts with a rice jacalin-related lectin to promote host colonization. *Plant Physiology* **179**: 1416-1430.

Hautea RA, Coffman WR, Sorrells ME, Bergstrom GC (1987) Inheritance of partial resistance to powdery mildew in spring wheat. *Theoretical and Applied Genetics* **73**: 609-615.

He J, Liu Y, Yuan D, Duan M, Liu Y, Shen Z, Yang C, Qiu Z, Liu D, Wen P *et al*. (2020) An R2R3 MYB transcription factor confers brown planthopper resistance by regulating the phenylalanine ammonia-lyase pathway in rice. *Proceedings of the National Academy of Sciences of the United States of America* **117**: 271-277.

Hurlburt NK, Chen LH, Stergiopoulos I, Fisher AJ (2018) Structure of the *Cladosporium fulvum* Avr4 effector in complex with $(GlcNAc)_6$ reveals the ligand-binding mechanism and uncouples its intrinsic function from recognition by the Cf-4 resistance protein. *PLoS Pathogens* **14**: e1007263.

Jashni MK, Mehrabi R, Collemare J, Mesarich CH, de Wit PJGM (2015) The battle in the apoplast: further insights into the roles of proteases and their inhibitors in plant-pathogen interactions. *Frontiers in Plant Science* **6:** 584.

Kamakura T, Yamaguchi S, Saitoh KI, Teraoka T, Yamaguchi I (2002) A novel gene, CBP1, encoding a putative extracellular chitin-binding protein, may play an important role in the hydrophobic surface sensing of *Magnaporthe grisea* during appressorium differentiation. *Molecular Plant-Microbe Intertations* **15**: 437-444.

Kuroki M, Okauchi K, Yoshida S, Ohno Y, Murata S, Nakajima Y, Nozaka A, Tanaka N, Nakajima M, Taguchi H *et al*. (2017) Chitin-deacetylase activity induces appressorium differentiation in the rice blast fungus *Magnaporthe oryzae*. *Scientific Reports* **7**: 9697.

Li H, Dong Z, Ma C, Xia Q, Tian X, Sehgal S, Koo DH, Friebe B, Ma P, Liu W (2020a) A spontaneous wheat-Aegilops longissima translocation carrying Pm66 confers resistance to powdery mildew. *Theoretical and Applied Genetics* **133**: 1149-1159.

Li M, Dong L, Li B, Wang Z, Xie J, Qiu D, Li Y, Shi W, Yang L, Wu Q, *et al*. (2020b) A CNL protein in wild emmer wheat confers powdery mildew resistance. *New Phytologist* **228**: 1027-1037.

Li Q, Niu Z, Bao Y, Tian Q, Wang H, Kong L, Feng D (2016) Transcriptome analysis of genes related to resistance against powdery mildew in wheat-Thinopyrum alien addition disomic line germplasm SN6306. *Gene* **590**: 5-17.

Love MI, Huber W, Anders S. 2014. Moderated estimation of fold change and dispersion for RNA-seq data with DESeq2. *Genome Biology* **15**: 550.

Lu P, Guo L, Wang Z, Li B, Li J, Li Y, Qiu D, Shi W, Yang L, Wang N *et al*. (2020) A rare gain of function mutation in a wheat tandem kinase confers resistance to powdery mildew. *Nature Communications* **11**: 680.

Niu N, Liang W, Yang X, Jin W, Wilson ZA, Hu J, Zhang D (2013) EAT1 promotes tapetal cell death by regulating aspartic proteases during male reproductive development in rice. *Nature Communications* **4**: 1445.

Norriss MG, Frost-Smith TJ, Sutherland JIM (2007) Increasing endophyte alkaloid expression in tall fescue by selecting for increased endophyte hyphal density. *Proceedings of the New Zealand Grassland Association* **69**: 197-200.

Nowara D, Gay A, Lacomme C, Shaw J, Ridout C, Douchkov D, Hensel G, Kumlehn J, Schweizer P (2010) HIGS: host-induced gene silencing in the obligate biotrophic fungal pathogen Blumeria graminis. *Plant Cell* **22**: 3130-41.

Panstruga R (2013) Establishing compatibility between plants and obligate biotrophic pathogens. *Current Opinion in Plant Biology* **6**: 320-326.

Prasad BD, Creissen G, Lamb C, Chattool BB (2009) Overexpression of rice (*Oryza sativa* L.) OsCDR1 leads to constitutive activation of defense responses in rice and Arabidopsis. *Molecular Plant-Microbe Intertations* **22**: 1635-1644.

Prasad BD, Creissen G, Lamb C, Chattoo BB (2010) Heterologous expression and characterization of recombinant OsCDR1, a rice aspartic proteinase involved in disease resistance. *Protein Expression and Purification* **72**: 169-174.

Rawlings ND, Barrett AJ (1995) Families of aspartic peptidases, and those of unknown catalytic mechanism. *Methods in Enzymology* **248**: 105-120.

Rawlings ND, Barrett AJ, Finn R (2016) Twenty years of the MEROPS database of proteolytic enzymes, their substrates and inhibitors. *Nucleic Acids Research* **44**: 343-350.

Shaner G (1973) Evaluation of slow-mildewing resistance of Knox wheat in the field. *Phytopathology* **63**: 867-872.

Shen XK, Ma LX, Zhong SF, Liu N, Zhang M, Chen WQ, Zhou YL, Li HJ, Chang ZJ, Li X, *et al*. (2015) Identification and genetic mapping of the putative *Thinopyrum intermedium*‐derived dominant powdery mildew resistance gene *PmL962* on wheat chromosome arm 2BS. *Theoretical and Applied Genetics* **128**:517-528.

Singh RP, Singh PK, Rutkoski J, Hodson DP, He X, Jørgensen LN, Hovmøller MS, Huerta-Espino J (2016) Disease impact on wheat yield potential and prospects of genetic control. *Annual Review of Phytopathology* **54**: 303-322.

Smigielski L, Aguilar GB, Kwaaitaal M, Zhang WJ, Thordal-Christensen H (2019) The isoelectric point of proteins influences their translocation to the extrahaustorial matrix of the barley powdery mildew fungus. *Cellular Microbiology* **21**: e13091.

Tian QJ, Song J, Yang YL, Xu T, Wang HG, Feng DS (2017) Cloning and Bioinformatics of *TiAP1* Gene from *Thinopyrum intermedium*. *Shandong Agricultural Science* **49**: 1-9.

Tsigos I, Bouriotis V (1995) Purification and characterization of chitin deacetylase from *Colletotrichum lindemuthianum*. *Journal of Biological Chemistry* **270**: 26286-26291.

Upadhya R, Baker LG, Lam WC, Specht CA, Donlin MJ, Lodge JK (2018) *Cryptococcus neoformans* Cda1 and its chitin deacetylase activity are required for fungal pathogenesis. *mBio* **9**: e02087-18.

Xia YJ, Suzuki H, Borevitz1 J, Blount J, Guo ZJ, Patel K, Dixon RA, Lamb C (2004) An extracellular aspartic protease functions in Arabidopsis disease resistance signaling. *EMBO Journal* **23**: 980-988.

Xia YQ, Ma ZC, Qiu M, Guo BD, Zhang Q, Jiang HB, Zhang BY, Lin YC, Xuan MR, Sun L, *et al*. (2020) N-glycosylation shields *Phytophthora sojae* apoplastic effector PsXEG1 from a specific host aspartic protease. *Proceedings of the National Academy of Sciences of the United States of America* **117**: 27685-27693.

Yang C, Yu Y, Huang J, Meng F, Pang J, Zhao Q, Islam MA, Xu N, Tian Y, Liu J (2019) Binding of the *Magnaporthe oryzae* chitinase MoChia1 by a rice tetratricopeptide

766 repeat protein allows free chitin to trigger immune responses. *Plant Cell* **31**: 172-
767 188.
768 Yang YL, Feng DS (2020) Genome-wide identification of the aspartic protease gene
769 family and their response under powdery mildew stress in wheat. *Molcular*
770 *Biology Reports* **47**: 8949-8961.
771 You XM, Fang H, Wang RY, Wang GL, Ning YS (2020) Phenylalanine ammonia lyases
772 mediate broad-spectrum resistance to pathogens and insect pests in plants. *Science*
773 *Bulletin* **65**: 1425-1427.
774 Yuan C, Li C, Yan L, Jackson AO, Liu Z, Han C, Yu J, Li D (2011) A high throughput
775 barley stripe mosaic virus vector for virus induced gene silencing in monocots and
776 dicots. *PLoS One* **6**: e26468.
777 Zhang Z, Henderson C, Perfect E, Carver TLW, Thomas BJ, Skamnioti P, Gurr SJ (2005)
778 Of genes and genomes, needles and haystacks: *Blumeria graminis* and
779 functionality. *Molecular Plant Pathology* **6**: 561-575.
780 Zhai K, Deng Y, Liang D, Tang J, Yan B, Yin X, Lin H, Chen F, Yang D, Xie Z *et al*.
781 (2019) RRM transcription factors interact with NLRs and regulate broad-spectrum
782 blast resistance in rice. *Molecular Cell* **74**: 996-1009.
783 Zhao Y, Park RD, Muzzarelli RA (2010) Chitin Deacetylases: Properties and
784 Applications. *Marine Drugs* **8**: 24-46.
785 Zhou S, Miao QX, Huang LL, Chen LH (2017) Research progress in hemicellulose-
786 based functional materials. *Chemistry and Industry of Forest Product*s **37**: 10-18.
787 Zhou X, Liao H, Chern M, Yin J, Chen Y, Wang J, Zhu X, Chen Z, Yuan C, Zhao W *et*
788 *al*. (2018) Loss of function of a rice TPR-domain RNA-binding protein confers
789 broad-spectrum disease resistance. *Proceedings of the National Academy of*
790 *Sciences of the United States of America* **115**: 3174-3179.
791
792
793
794
795
796
797

798 **FIGURE LEGENDS**

799 Fig. 1 qRT-PCR and VIGS analysis of the *TiAP1* effect on the *Bgt* resistance. (A)
800 Expression levels of *TiAP1* in YN15 and SN6306 that were induced by *Bgt*. Total
801 RNA from the leaves of YN15 and SN6306 that were induced by *Bgt* at 0, 12, 24,

802 48, 72, and 96 h were extracted as the template to be detected by qRT-PCR. Data
803 represent mean ± S.D. of n = 3 technical replicates. (B) Relative quantification of
804 expression levels of *TiAP1*. Total RNA from the leaves of barley stripe mosaic
805 virus (BSMV):00 and BSMV: TiAP1as inoculated with *E09* for ten days were
806 extracted as the template for the detection by qRT-PCR. (C) Disease phenotype of
807 the BSMV:00 and BSMV: TiAP1as inoculated with *E09*. Photographs were taken
808 at 10 dpi. (D) Microscopic observation of the disease symptoms of BSMV:00 and
809 BSMV: TiAP1as 10 dpi. Bar = 100 μm.

810 Fig. 2 The TiAP1 prokaryotic expression and purification, and the reduction of the
811 powdery mildew severity (lesions area) on the wheat seedlings by a recombination
812 protein treatment. (A) The TiAP1 protein expression detection by western blotting
813 before and after induction. M: Pre-stained protein ladder; Lane1: Supernatant of
814 non-induced; Lane 2: Subside of non-induced; Lane 3: Supernatant of induced;
815 Lane 4: Subside of induced. (B) SDS-PAGE analysis of the inclusion body
816 purification. M: Low-molecular weight protein ladder; Lane 1: Inclusions after
817 dissolving the centrifugal supernatant; Lane 2: The effluent of supernatant was
818 incubated with nickel iminodiacetic acid (Ni-IDA); Lane 3-6: The effluent of the
819 imidazole elution of 50 mM; Lane 7-11: The effluent of the imidazole elution of
820 100 mM; Lane 12-13: The effluent of the imidazole elution of 300 mM; (C) TiAP1
821 quality assurance after renaturation. M: Pre-stained protein ladder; Lane 1: TiAP1
822 protein (1.5 μg). (D) Disease phenotype of YN15 smeared with TiAP1 and the tag
823 protein from pET28a (CK) when inoculated with *E09* for five days. (E)
824 Microscopic (Nikon Ni-U, Japan) analysis of the disease symptoms of YN15
825 smeared with TiAP1 and CK when inoculated with *E09* for five days. Bar = 100
826 μm. (F) The proportion of lesions in the leaf area of YN15 that was pre-treated
827 with the recombinant TiAP1 five days before *Bgt E09* inoculation relative to the
828 control. Control: Pre-treated with the purified recombinant label protein from the
829 pET28a construct. Different letters above the bars indicate statistically significant
830 differences (P <0.05) as obtained by one-way analysis of variance with least

831 significance difference and Duncan's multiple range test method.

832 Fig. 3 Identifying the resistance of transgenic *TiAP1* wheat. (A) Expression levels of
833 *TiAP1* in Bobwhite and the transgenic Bobwhite with *TiAP1* when inoculated with
834 *E09* for two days. (B) Disease phenotype of Bobwhite and the transgenic Bobwhite
835 with *TiAP1* when inoculated with *E09* for five days. (C) Microscopic (Nikon Ni-
836 U, Japan) analysis of the disease symptoms of Bobwhite and the transgenic
837 Bobwhite with *TiAP1* when inoculated with *E09* for two days. Bar = 100 μm. (D)
838 Count of *Bgt* conidia in different stages of the *Bgt* when inoculated with *E09* for
839 two days in Bobwhite and the transgenic Bobwhite with *TiAP1*. (E) The HI
840 statistics of the *Bgt* when inoculated with *E09* for two days in Bobwhite and the
841 transgenic Bobwhite with *TiAP1*. Different letters above the bars indicate
842 statistically significant differences (P <0.05) as obtained by one-way analysis of
843 variance with least significance difference and Duncan's multiple range test
844 method. (F) Identifying the resistance of different wheat at the adult stage natural
845 infected by powdery mildew in the glasshouse. (1) Bobwhite; (2) The transgenic
846 Bobwhite with *TiAP1*; (3) YN15; (4) F_1 obtained from cross breeding between
847 YN15 and homozygous transgenic *TiAP1* Bobwhite.

848 Fig. 4 Subcellular localisation of the fusion protein. (A) Confocal laser scanning
849 microscopy (Leica SP5 - X, Germany) observation of the leaf epidermal cells
850 revealed that Δsp-TiAP-GFP appears to be localised in the cytoplasm, while
851 TiAP1-GFP is predominantly localised in the extracellular region, where white
852 arrows indicate plasmolysis and the yellow dotted line shows the location of the
853 cell membrane of the two adjacent cells. A GFP signal was used as the control. Bar
854 = 20 μm. (B) The enlargement of the blue box in TiAP1-GFP. (C) The enlargement
855 of the blue box in Δsp-TiAP1-GFP. （D）*B. graminis* f. sp. *hordei* induced the
856 accumulation of TiAP1-mYFP and mCherry-TaSYP51 at the infection site. This
857 figure is part of Video S1. Bar = 20 μm.

858 Fig. 5 Interaction *in vitro* and *in vivo* of TiAP1 with BgtCDA1. (A) Yeast two-hybrid
859 analysis of the interaction between TiAP1 and BgtCDA1. Yeasts expressing the

860 interacting combinations of bait and prey were spotted on the SD-HAWL/X-α-
861 Gal/ABA. Bait-53 and AD-T (prey) were the positive controls, while Bait-Lam
862 and AD-T as well as Bait-BD and AD-BgtCDA1 were used as the negative
863 controls. (B) Luciferase complementation imaging assay showing that TiAP1
864 interacted with and BgtCDA1. The ΔspTiAP1-nLuc and cLuc-ΔspBgtCDA1 were
865 transiently co-expressed in *N. benthamiana*. Co-infiltration of cLuc/nLuc-tagged
866 ΔspTiAP1 protein with the nLuc/cLuc-tagged ΔspBgtCDA1 or the empty vectors
867 were used as negative controls, where the images were observed using
868 chemiluminescence imaging two days later. (C) The Co-IP analysis between
869 TiAP1 and BgtCDA1. (D) Bimolecular florescent complimentary assay showing
870 TiAP1 interaction with BgtCDA1. The cGFP-ΔspTiAP1 and nGFP-ΔspBgtCDA1
871 were transiently co-expressed in *N. benthamiana*. Co-infiltrations of nGFP/cGFP-
872 ΔspTiAP1, cGFP/nGFP- ΔspBgtCDA1, or the empty vectors group nGFP/cGFP
873 were used as negative controls. The positive controls were nYFP-14-3-3/14-3-3-
874 cCFP. The green florescent protein (GFP) signal was visualised using confocal
875 microscopy (Leica SP5 - X, Germany). Bar = 20 μm.

876 Fig. 6 The silencing of *BgtCDA1* reduced *Bgt* infection. (A) Wheat YN15 leaves,
877 bombarded with RNAi and GUS reporter constructs, were infected with *Bgt* and
878 calculated for fungal haustorial index. The haustorial index was calculated as the
879 ratio of haustoria-containing transformed cells (GUS expressing cells) divided
880 by the total number of transformed cells. Data shown are mean values, $n = 4$, and
881 a minimum of 150 transformed cells were counted in each repeat. Relative
882 haustorial index was computed relative to the empty vector pIPKTA30N control
883 of each experiment, which was set to 100%. The Mlo-RNAi was as another
884 control. Different letters above the bars indicate statistically significant
885 differences ($P < 0.05$) as obtained by one-way analysis of variance with least
886 significance difference and Duncan's multiple range test method. Arrow
887 indicates haustorium. Bar = 20 μm. (B) Wheat YN15 leaves, bombarded with
888 RNAi and GUS reporter constructs, were infected with *Bgt.* Arrow indicates

889 haustoria. Bar = 20 μm. (C) Disease phenotype of the BSMV:00 and BSMV:
890 BgtCDA1as inoculated with *E09*. Photographs were taken at 5 dpi. (D)
891 Microscopic observation of the disease symptoms of BSMV:00 and BSMV:
892 BgtCDA1as 3 dpi using *E09*. Bar = 100 μm. (E) The proportion of lesions in the
893 leaf area of BSMV:00 and BSMV: BgtCDA1as inoculated with *E09* five days.
894 (F) The hyphal density score of leaf material in BSMV:00 and BSMV:
895 BgtCDA1as 3 dpi using *E09* in microscopic observation field plots. Different
896 letters above the bars indicate statistically significant differences (P <0.05) as
897 obtained by one-way analysis of variance with least significance difference and
898 Duncan's multiple range test method.

899 Fig. 7 The transcriptome and qRT-PCR analysis of the transgenic wheat with *TiAP1*.
900 (A) Heat map of selected pathogen-responsive genes in Bobwhite without and
901 with induction of *Bgt* for two days (Bob-0 and Bob-2, respectively), and
902 overexpression line OE2 as the same treatment (OE2-0 and OE2-2, respectively).
903 (B) qRT-PCR analysis of the differential expression gene *TraesCS1B02G440300*,
904 *TraesCS2A02G161500*, *TraesCS2A02G199300*, *TraesCS3B02G379200*,
905 *TraesCS5D02G188600*, *TraesCS5A02G049600*, *TraesCS3B02G259500*,
906 *TraesCS2B02G224300*, *TraesCS6A02G266100*, *TraesCS2D02G099900*,
907 *TraesCS6B02G018700* and *TraesCS2B02G529400* of selected induced of *Bgt* for
908 two days.

909 Fig. 8 A proposed model of the TiAP1 interaction with chitin deacetylase to increase
910 the resistance to *Bgt* in wheat. (A) The *Bgt* cell walls were targeted by wheat-
911 secreted chitinases to release the chitin fragments that can further activate the host
912 immune system. (B) *Bgt* would secrete BgtCDA1 to convert the cell wall chitin
913 into chitosan, while the host invasion may protect the hyphae of the pathogenic
914 fungi from being hydrolysed by the extracellular plant chitinases, thereby
915 protecting the integrity of the fungal cell wall and inhibiting the resistance
916 response mechanism of the plant. (C) Interaction between TiAP1 and BgtCDA1
917 in the transgenic *TiAP1* gene wheat, causing BgtCDA1 to inactivate its

deacetylation function, therefore the chitin in fungal cell walls would be targeted by the wheat-secreted chitinases that liberate chitin the fragments that can further activate the host immune system. When the transgenic *TiAP1* wheat was infected by powdery mildew, the hormone signals related gene expression *in vivo* would interact to activate plant disease resistance and upregulate the expression of phenylalanine ammonia lyases in the lignin biosynthesis and XTH30 in the xylan metabolism of the transgenic *TiAP1* wheat. Hence, it enhances the ability of the plant cell walls to resist the penetration by pathogens.

Supporting Informations

Short Legends

Fig. S1 The TiAP1 prokaryotic expression and purification.

Fig. S2 Identification of the transgenic Bobwhite with the *TiAP1* gene and the subsequent hybrid generation.

Fig. S3 Validation of wheat powdery mildew resistance in the representative hybrid subsequent generation of F_3, which showed resistance to *E09* at 7 dpi in the seedling stage.

Fig. S4 Validation of the wheat powdery mildew resistance in 7 transgenic wheats Bobwhite with the *TiAP1* gene in the adult stage, which showed high resistance to powdery mildew.

Fig. S5 Subcellular localisation of the fusion protein in the *N. benthamiana* leaf epidermal cells.

Fig. S6 The BgtCDA1 protein bioinformatics analysis.

Fig. S7 Transcriptome analysis of the *TiAP1* and *BgtCDA1* co-regulated genes.

Methods S1 Additional description of methods.

Table S1 Evaluation of the resistance to *E09* in YN15, wheat lines overexpressing *TiAP1*, and the hybrid subsequent generation of F_3 in the seedling stage.

Table S2 Evaluation of the resistance to powdery mildew in Bobwhite and wheat lines overexpressing *TiAP1* at the adult stage.

Table S3 Differential gene expression in the transgenic overexpression line OE2 and Bobwhite when inoculated with *E09* for two days.

Table S4 Gene ontology (GO) analysis of the differentially expressed genes in OE2-2 and Bob-2.

Table S5 Expression of selected pathogen-responsive genes in Bob-0, Bob-2, OE2-0, and OE2-2 in the RNA-Seq experiments.

Table S6 The primers used in this study.

Video S1 Confocal microscopy (Leica SP5 - X, Germany) z-scan image series of TiAP-mYFP/mCherry-TaSYP51 on barley leaf epidermic cell under the infection of *Bgh*.

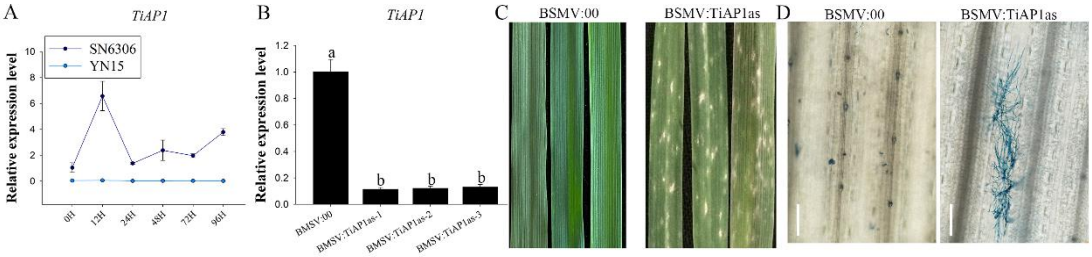

Fig. 1 qRT-PCR and VIGS analysis of the *TiAP1* effect on the *Bgt* resistance. (A) Expression levels of *TiAP1* in YN15 and SN6306 that were induced by *Bgt*. Total RNA from the leaves of YN15 and SN6306 that were induced by *Bgt* at 0, 12, 24, 48, 72, and 96 h were extracted as the template to be detected by qRT-PCR. Data represent mean ± S.D. of $n = 3$ technical replicates. (B) Relative quantification of expression levels of *TiAP1*. Total RNA from the leaves of barley stripe mosaic virus (BSMV):00 and BSMV: TiAP1as inoculated with *E09* for ten days were extracted as the template for the detection by qRT-PCR. (C) Disease phenotype of the BSMV:00 and BSMV: TiAP1as inoculated with *E09*. Photographs were taken at 10 dpi. (D) Microscopic observation of the disease symptoms of BSMV:00 and BSMV: TiAP1as 10 dpi. Bar = 100 μm.

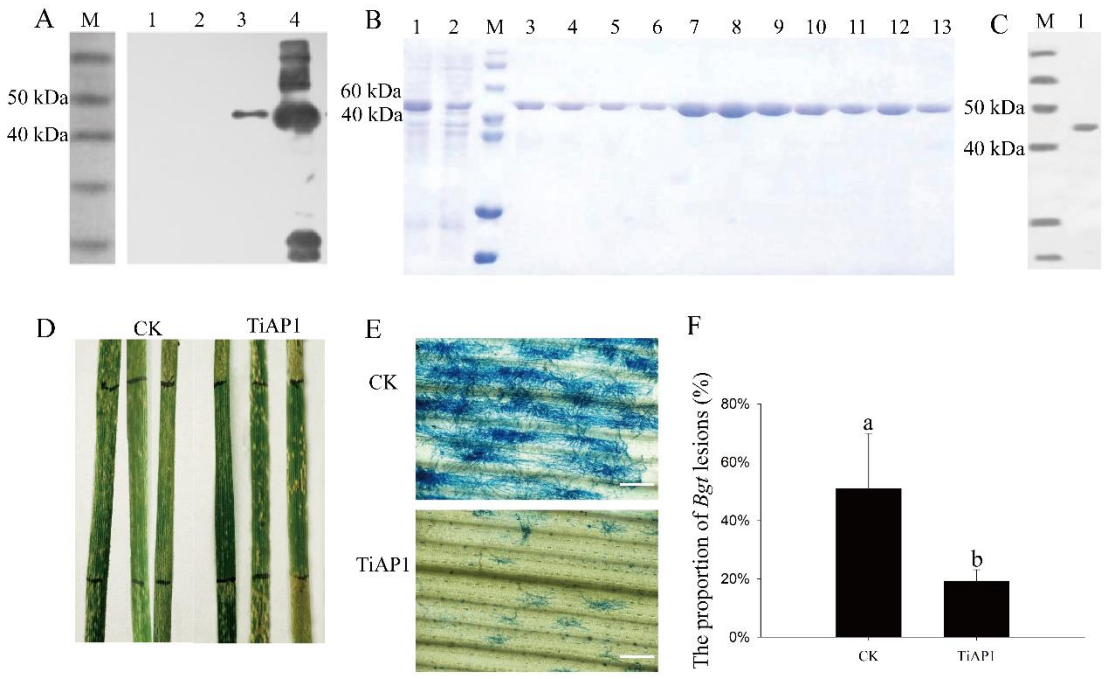

Fig. 2 The TiAP1 prokaryotic expression and purification, and the reduction of the powdery mildew severity (lesions area) on the wheat seedlings by a recombination protein treatment. (A) The TiAP1 protein expression detection by western blotting before and after induction. M: Pre-stained protein ladder; Lane1: Supernatant of non-induced; Lane 2: Subside of non-induced; Lane 3: Supernatant of induced; Lane 4: Subside of induced. (B) SDS-PAGE analysis of the inclusion body purification. M: Low-molecular weight protein ladder; Lane 1: Inclusions after dissolving the centrifugal supernatant; Lane 2: The effluent of supernatant was incubated with nickel iminodiacetic acid (Ni-IDA); Lane 3-6: The effluent of the imidazole elution of 50 mM; Lane 7-11: The effluent of the imidazole elution of 100 mM; Lane 12-13: The effluent of the imidazole elution of 300 mM; (C) TiAP1 quality assurance after renaturation. M: Pre-stained protein ladder; Lane 1: TiAP1 protein (1.5 μg). (D) Disease phenotype of YN15 smeared with TiAP1 and the tag protein from pET28a (CK) when inoculated with *E09* for five days. (E) Microscopic (Nikon Ni-U, Japan) analysis of the disease symptoms of YN15 smeared with TiAP1 and CK when inoculated with *E09* for five days. Bar = 100 μm. (F) The proportion of lesions in the leaf area of YN15 that was pre-treated with the recombinant TiAP1 five days before *Bgt E09* inoculation relative to the control. Control: Pre-treated with the purified recombinant label protein from the pET28a construct. Different letters above the bars indicate statistically significant differences (P <0.05) as obtained by one-way analysis of variance with least significance difference and Duncan's multiple range test method.

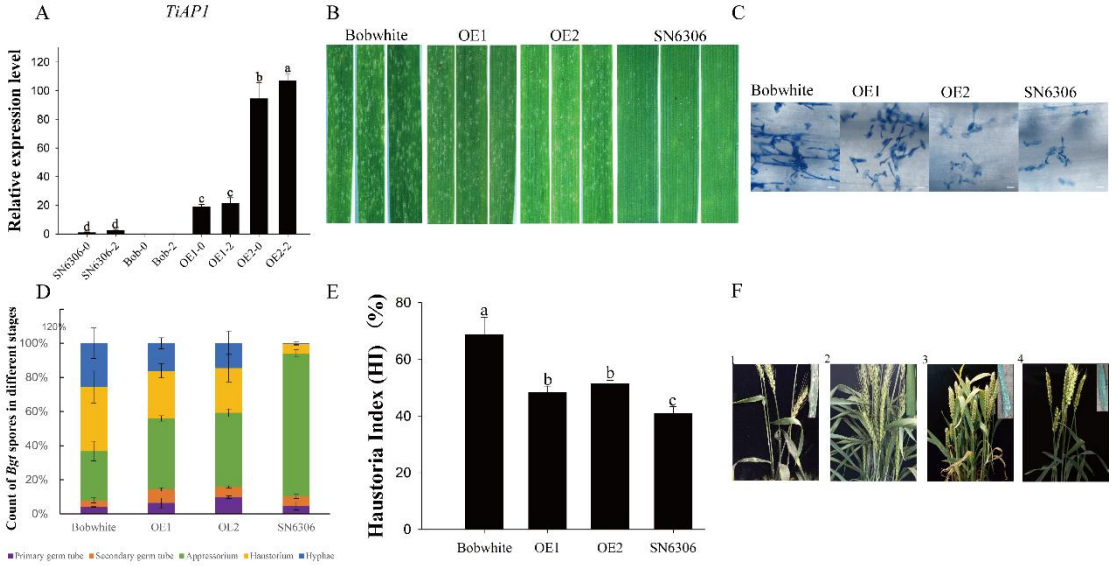

Fig. 3 Identifying the resistance of transgenic *TiAP1* wheat. (A) Expression levels of *TiAP1* in Bobwhite and the transgenic Bobwhite with *TiAP1* when inoculated with *E09* for two days. (B) Disease phenotype of Bobwhite and the transgenic Bobwhite with *TiAP1* when inoculated with *E09* for five days. (C) Microscopic (Nikon Ni-U, Japan) analysis of the disease symptoms of Bobwhite and the transgenic Bobwhite with *TiAP1* when inoculated with *E09* for two days. Bar = 100 μm. (D) Count of *Bgt* conidia in different stages of the *Bgt* when inoculated with *E09* for two days in Bobwhite and the transgenic Bobwhite with *TiAP1*. (E) The HI statistics of the *Bgt* when inoculated with *E09* for two days in Bobwhite and the transgenic Bobwhite with *TiAP1*. Different letters above the bars indicate statistically significant differences (P <0.05) as obtained by one-way analysis of variance with least significance difference and Duncan's multiple range test method. (F) Identifying the resistance of different wheat at the adult stage natural infected by powdery mildew in the glasshouse. (1) Bobwhite; (2) The transgenic Bobwhite with *TiAP1*; (3) YN15; (4) F_1 obtained from cross breeding between YN15 and homozygous transgenic *TiAP1* Bobwhite.

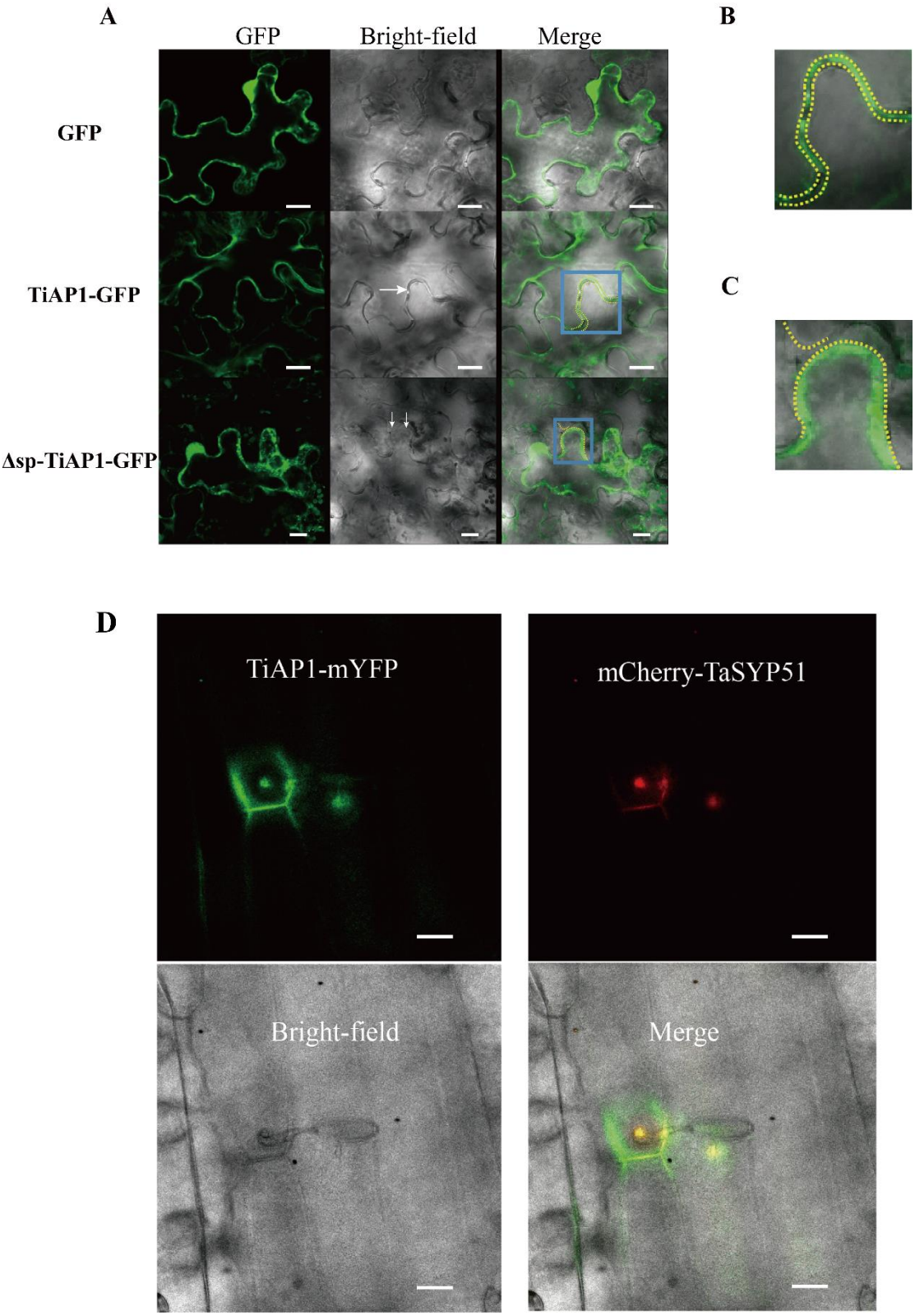

1053

1054

1055

1056

1057

Fig. 4 Subcellular localisation of the fusion protein. (A) Confocal laser scanning microscopy (Leica SP5 - X, Germany) observation of the leaf epidermal cells revealed that Δsp-TiAP-GFP appears to be localised in the cytoplasm, while TiAP1-GFP is predominantly localised in the extracellular region, where white arrows indicate plasmolysis and the yellow dotted line shows the location of the cell membrane of the two adjacent cells. A GFP signal was used as the control. Bar = 20 μm. (B) The enlargement of the blue box in TiAP1-GFP. (C) The enlargement of the blue box in Δsp-TiAP1-GFP. (D) *B. graminis* f. sp. *hordei* induced the accumulation of TiAP1-mYFP and mCherry-TaSYP51 at the infection site. This figure is part of Video S1. Bar = 20 μm.

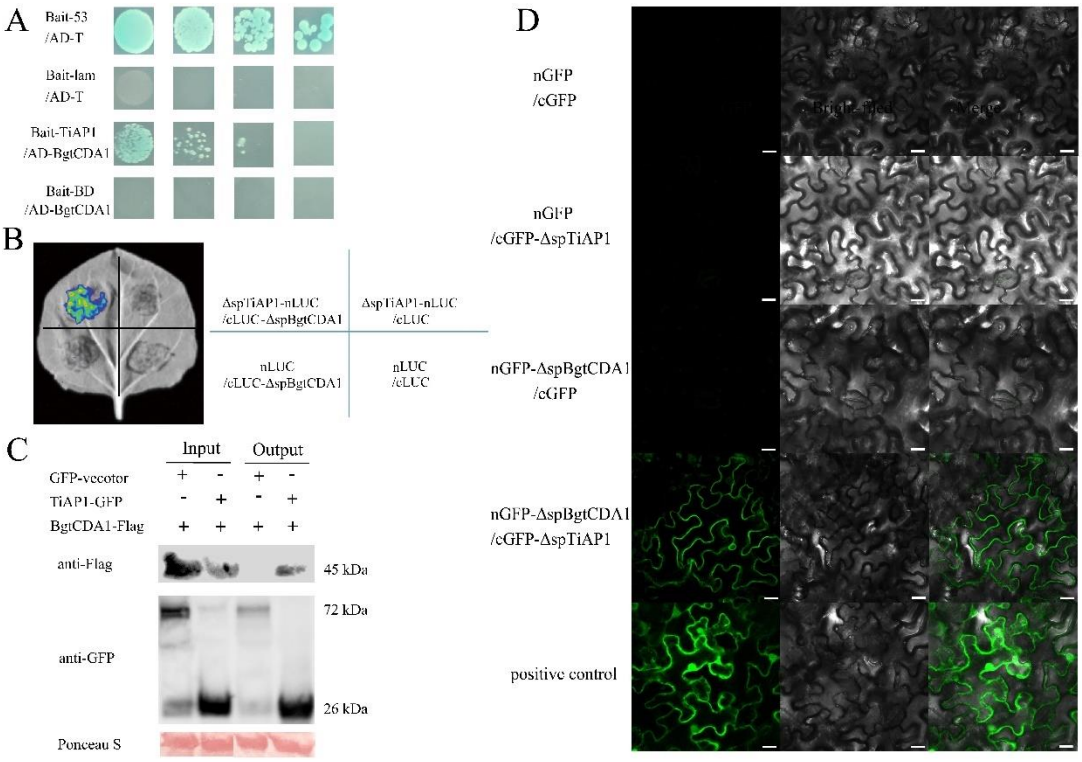

Fig. 5 Interaction *in vitro* and *in vivo* of TiAP1 with BgtCDA1. (A) Yeast two-hybrid analysis of the interaction between TiAP1 and BgtCDA1. Yeasts expressing the interacting combinations of bait and prey were spotted on the SD-HAWL/X-α-Gal/ABA. Bait-53 and AD-T (prey) were the positive controls, while Bait-Lam and AD-T as well as Bait-BD and AD-BgtCDA1 were used as the negative controls. (B) Luciferase complementation imaging assay showing that TiAP1 interacted with and BgtCDA1. The ΔspTiAP1-nLuc and cLuc-ΔspBgtCDA1 were transiently co-expressed in *N. benthamiana*. Co-infiltration of cLuc/nLuc-tagged ΔspTiAP1 protein with the nLuc/cLuc-tagged ΔspBgtCDA1 or the empty vectors were used as negative controls, where the images were observed using chemiluminescence imaging two days later. (C) Bimolecular florescent complimentary assay showing TiAP1 interaction with BgtCDA1. The cGFP-ΔspTiAP1 and nGFP-ΔspBgtCDA1 were transiently co-expressed in *N. benthamiana*. Co-infiltrations of nGFP/cGFP-ΔspTiAP1, cGFP/nGFP-ΔspBgtCDA1, or the empty vectors group nGFP/cGFP were used as negative controls. The positive controls were nYFP-14-3-3/14-3-3-cCFP. The green florescent protein (GFP) signal was visualised using confocal microscopy (Leica SP5 - X, Germany). Bar = 20 μm.

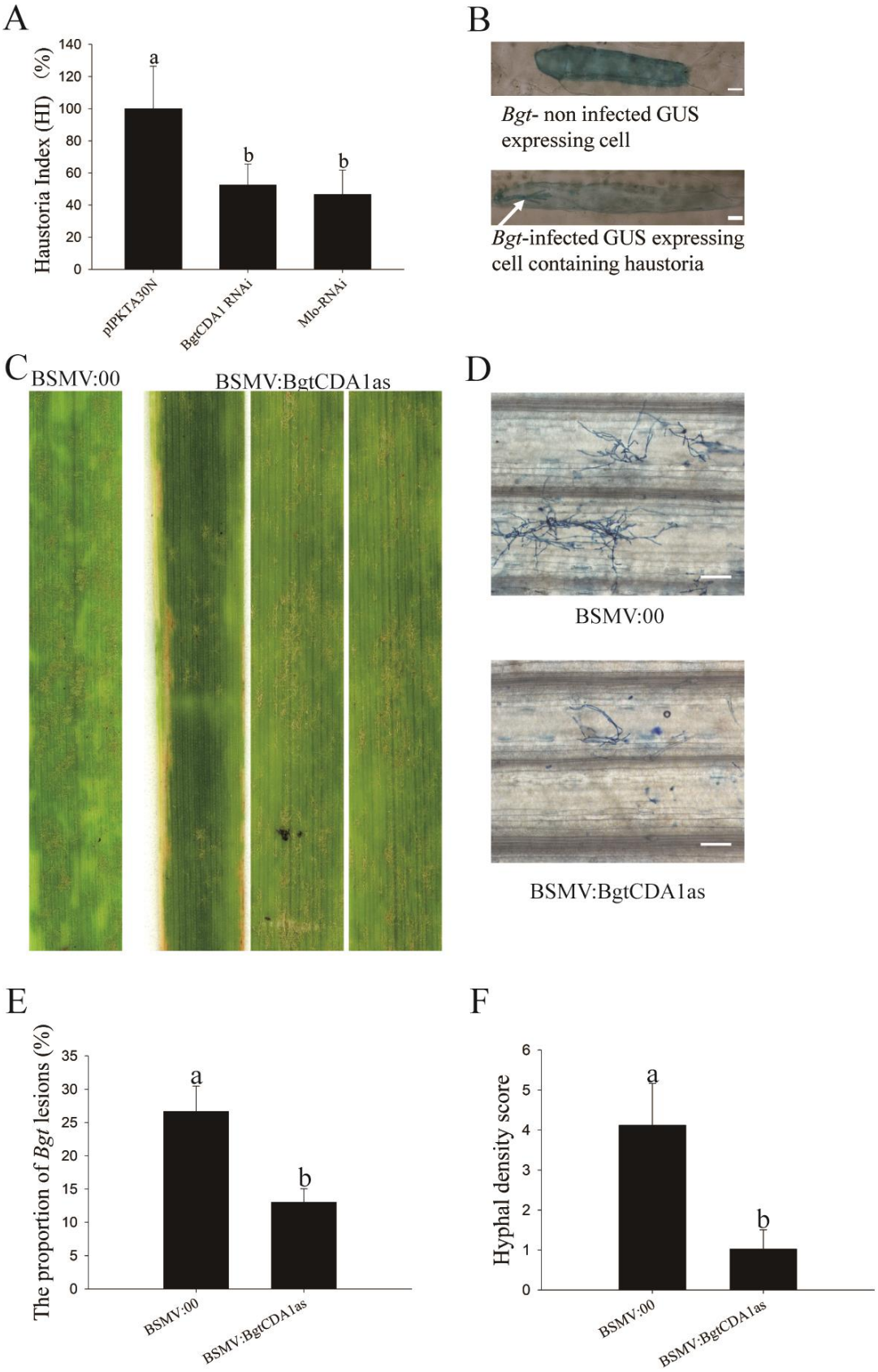

1120

1121

1122

1123 Fig. 6 The silencing of *BgtCDA1* reduced *Bgt* infection. (A) Wheat YN15 leaves,
1124 bombarded with RNAi and GUS reporter constructs, were infected with *Bgt* and
1125 calculated for fungal haustorial index. The haustorial index was calculated as the
1126 ratio of haustoria-containing transformed cells (GUS expressing cells) divided
1127 by the total number of transformed cells. Data shown are mean values, $n = 4$, and
1128 a minimum of 150 transformed cells were counted in each repeat. Relative
1129 haustorial index was computed relative to the empty vector pIPKTA30N control
1130 of each experiment, which was set to 100%. The Mlo-RNAi was as another
1131 control. Different letters above the bars indicate statistically significant
1132 differences ($P < 0.05$) as obtained by one-way analysis of variance with least
1133 significance difference and Duncan's multiple range test method. Arrow
1134 indicates haustorium. Bar = 20 μm. (B) Wheat YN15 leaves, bombarded with
1135 RNAi and GUS reporter constructs, were infected with *Bgt.* Arrow indicates
1136 haustoria. Bar = 20 μm. (C) Disease phenotype of the BSMV:00 and BSMV:
1137 BgtCDA1as inoculated with *E09*. Photographs were taken at 5 dpi. (D)
1138 Microscopic observation of the disease symptoms of BSMV:00 and BSMV:
1139 BgtCDA1as 3 dpi using *E09*. Bar = 100 μm. (E) The proportion of lesions in the
1140 leaf area of BSMV:00 and BSMV: BgtCDA1as inoculated with *E09* five days.
1141 (F) The hyphal density score of leaf material in BSMV:00 and BSMV:
1142 BgtCDA1as 3 dpi using *E09* in microscopic observation field plots. Different
1143 letters above the bars indicate statistically significant differences ($P < 0.05$) as
1144 obtained by one-way analysis of variance with least significance difference and
1145 Duncan's multiple range test method.
1146
1147
1148
1149
1150
1151
1152
1153
1154
1155
1156
1157
1158
1159
1160
1161

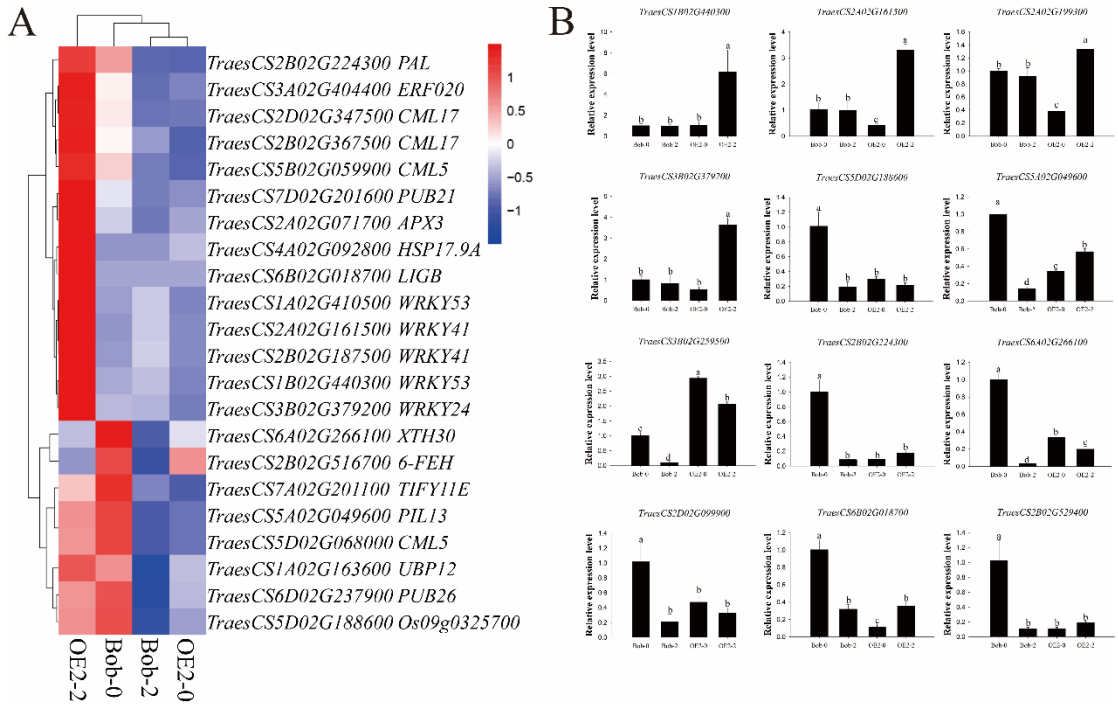

Fig. 7 The transcriptome and qRT-PCR analysis of the transgenic wheat with *TiAP1*. (A) Heat map of selected pathogen-responsive genes in Bobwhite without and with induction of *Bgt* for two days (Bob-0 and Bob-2, respectively), and overexpression line OE2 as the same treatment (OE2-0 and OE2-2, respectively). (B) qRT-PCR analysis of the differential expression gene *TraesCS1B02G440300*, *TraesCS2A02G161500*, *TraesCS2A02G199300*, *TraesCS3B02G379200*, *TraesCS5D02G188600*, *TraesCS5A02G049600*, *TraesCS3B02G259500*, *TraesCS2B02G224300*, *TraesCS6A02G266100*, *TraesCS2D02G099900*, *TraesCS6B02G018700* and *TraesCS2B02G529400* of selected induced of *Bgt* for two days.

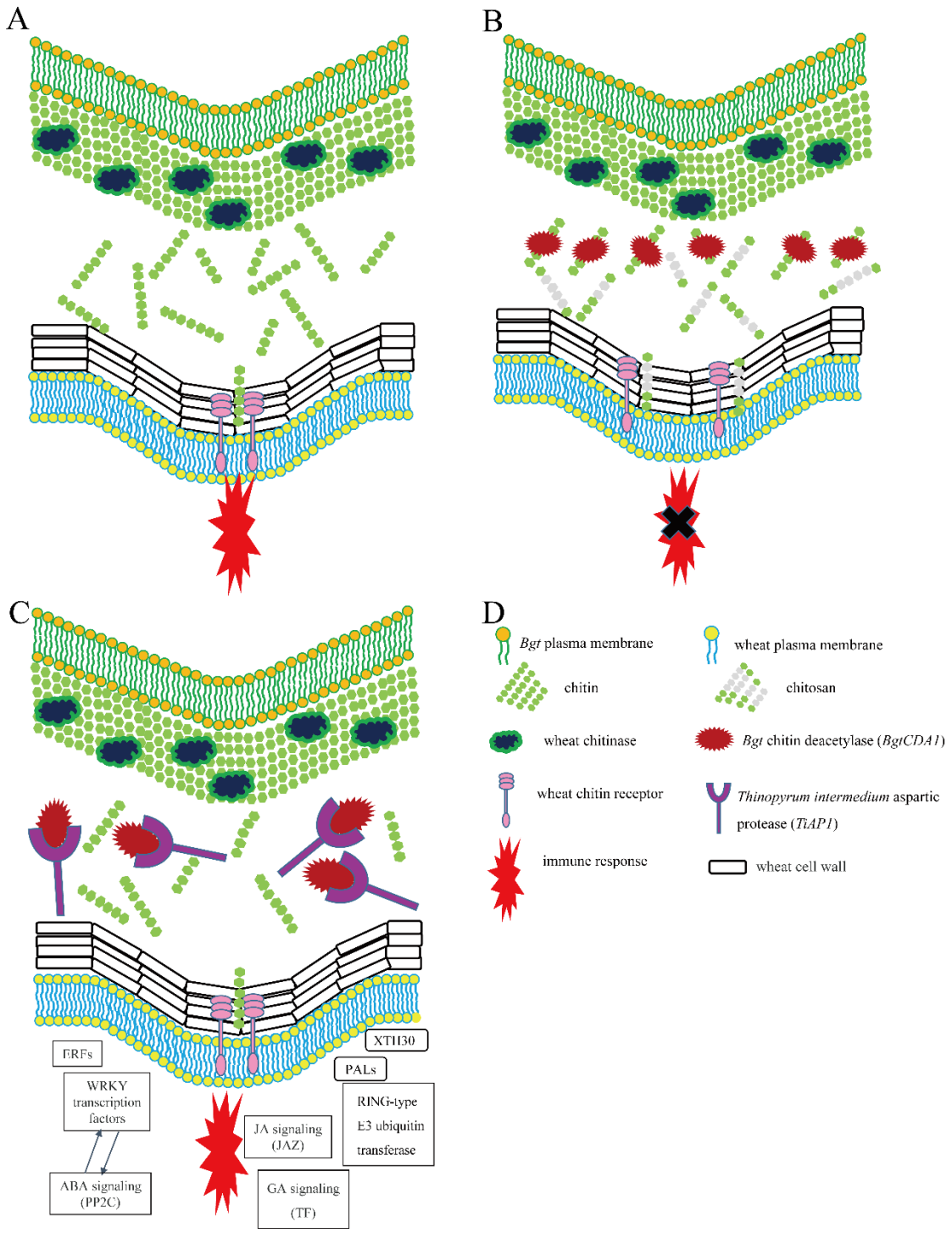
A
B
C
D
Bgt plasma membrane
wheat plasma membrane
chitin
chitosan
wheat chitinase
Bgt chitin deacetylase (BgtCDA1)
wheat chitin receptor
Thinopyrum intermedium aspartic protease (TiAP1)
immune response
wheat cell wall
ERFs
WRKY transcription factors
ABA signaling (PP2C)
JA signaling (JAZ)
GA signaling (TF)
XTH30
PALs
RING-type E3 ubiquitin transferase

1195 Fig. 8 A proposed model of the TiAP1 interaction with chitin deacetylase to increase
1196 the resistance to *Bgt* in wheat. (A) The *Bgt* cell walls were targeted by wheat-
1197 secreted chitinases to release the chitin fragments that can further activate the host
1198 immune system. (B) *Bgt* would secrete BgtCDA1 to convert the cell wall chitin
1199 into chitosan, while the host invasion may protect the hyphae of the pathogenic
1200 fungi from being hydrolysed by the extracellular plant chitinases, thereby
1201 protecting the integrity of the fungal cell wall and inhibiting the resistance
1202 response mechanism of the plant. (C) Interaction between TiAP1 and BgtCDA1
1203 in the transgenic *TiAP1* gene wheat, causing BgtCDA1 to inactivate its
1204 deacetylation function, therefore the chitin in fungal cell walls would be targeted
1205 by the wheat-secreted chitinases that liberate chitin the fragments that can further
1206 activate the host immune system. When the transgenic *TiAP1* wheat was infected
1207 by powdery mildew, the hormone signals related gene expression *in vivo* would
1208 interact to activate plant disease resistance and upregulate the expression of
1209 phenylalanine ammonia lyases in the lignin biosynthesis and XTH30 in the xylan
1210 metabolism of the transgenic *TiAP1* wheat. Hence, it enhances the ability of the
1211 plant cell walls to resist the penetration by pathogens.